Computers & Operations Research 138 (2022) 105602

Contents lists available at ScienceDirect

Computers and Operations Research

journal homepage: www.elsevier.com/locate/cor

# Integration of turnaround and aircraft recovery to mitigate delay propagation in airline networks

Jan Evler *, Martin Lindner, Hartmut Fricke, Michael Schultz

*Institute of Logistics and Aviation, Technische Universität Dresden, Hettnerstr. 1-3, 01069 Dresden, Germany*

ARTICLE INFO

*Keywords:*
Airline schedule recovery
Airline ground operations
Delay propagation
Heterogeneous VRPTW
Time-continuous RCPSP

ABSTRACT

This article presents a novel approach to incorporate the aircraft turnaround, which has recently been identified as one of the major contributors to airline delay, into existing concepts for integrated aircraft, crew, and passenger recovery. We aim to fill the research gap on how to holistically model network delay propagation as tactical decision support for airline schedule recovery. Our model introduces a heterogeneous vehicle routing problem with time windows for the assignment of aircraft to flight routes and integrates it with an extended version of the resource-constrained project schedule problem for the allocation of scarce resources to turnarounds at the central hub airport, such that we can proactively estimate delay propagation in an airline network. Passenger and crew itineraries are modelled as links between flights, such that needed transfer times influence the stand allocation and resource assignment. These links may only be broken if reserve capacities are available and the related rebooking and compensation costs are more efficient than accepting departure delays to maintain transfers. With this approach, we are able to calculate flight-specific delay cost functions and find substantial dependencies about the time of the day, the number of succeeding flight legs and particular downstream destinations.

The integrated recovery model is implemented into a rolling horizon algorithm and applied to a case study setting to analyse its performance in comparison to the individual turnaround and aircraft recovery models. Within different delay scenarios, we find that the incorporation of turnaround recovery options significantly improves the resilience of the airline network. Especially in low and moderate delay situations, we achieve a full recovery of the flight schedule simply by rebooking passengers, reallocating aircraft among stands and accelerating ground operations. Thus, often considered recovery options, such as aircraft swaps and flight cancellations, are not required for delays around 30 min in our case study. This reduces total costs in comparison to the conventional aircraft recovery model by 49%. Despite the lower efficiency of turnaround recovery in medium and high delay scenarios, the combination of flexible aircraft assignments and ground operations still generates additional cost savings of at least 21% and helps to reduce the necessary amount of optimal recovery options.

## 1. Introduction

Schedule recovery is a vital element in daily airline operations, given that many stochastic influences, such as weather, traffic, unscheduled maintenance or unpredictable ("irrational") human behaviour frequently cause deviations to the initial flight schedule. Knowing the high economic pressure in the airline industry, network planners constantly aim at finding an efficient balance between operational robustness (i.e., assign schedule buffers to mitigate disturbances or stochastic deviations) and schedule profitability (i.e., maximize aircraft "air-time" while granting network connectivity) (Wu, 2016). Consequently, many airlines have implemented hub and spoke operations to profit from economies of scale and scope (Bryan and O'Kelly, 1999), such that ground and maintenance services are operated at a central (hub) airport, where only two additional flights are necessary to connect a new destination to the entire network.

In order to facilitate an attractive passenger product with high connectivity and short transfer times between flights at the hub, many aircraft need to arrive and depart within a short time window, creating so-called "hub banks". The availability of many aircraft at the hub at the same time holds flexibility to reallocate aircraft to flight legs if schedule disturbances occur. However, such densely scheduled operations naturally cause dependencies, which may be attributed to the constrained airport infrastructure and resource availability. With 32.6%, ground operations are the primary source of departure delay

* Corresponding author.
*E-mail address:* jan.evler@tu-dresden.de (J. Evler).

https://doi.org/10.1016/j.cor.2021.105602
Received 19 March 2021; Received in revised form 11 October 2021; Accepted 11 October 2021
Available online 16 October 2021
0305-0548/

in Europe, only topped by a 44% contribution of reactionary delay, which is by definition secondary delay and might partially be the spill over effect generated by a primary delay at previous airports in the daily aircraft rotation. In Europe in 2019, average departure delay has accumulated to 12.8 min per flight and has caused more than 22% of all flights to obtain arrival delays larger than 15 min (Eurocontrol, 2020). Despite lower traffic volumes and better on-time performances during the Covid-19 pandemic, cost pressure on airlines has even increased, such that future airline operations concepts should aim at minimizing delay impacts from ground operations onto the network.

### 1.1. State-of-the-art in Tactical Airline Schedule Recovery

A profitable airline schedule can hardly set aside enough absorptive capacities to account for all potential delays throughout an entire flight plan period. Although much academic attention has focused on the efficient allocation of schedule buffers (Stojković et al., 2002; AhmadBeygi et al., 2010a; Burke et al., 2010; Dück et al., 2012; Aloulou et al., 2013; Safak et al., 2017) and the identification of weak links in a planned schedule based on historical flight data (Rosenberger et al., 2002; AhmadBeygi et al., 2008; Wu and Law, 2019), non of these have found a way to entirely supersede schedule recovery at tactical level (i.e., on the day of operations) without compromising profitability. Thus, airlines have established Airline Operations Control Center (AOCC) for the tactical monitoring and appropriate adjustment of their schedules if needed. The typical AOCC control loop is so far still operated manually, such that AOCC controllers need to frequently check for schedule deviations (delay) or airport/airspace constraints requiring corrective actions. The triggers for such assessments are predefined in the internal recovery policy, which typically contain delay thresholds or department-specific performance targets. Once recovery actions are required, adopted schedules are generated separately per airline department relying on expert knowledge held by the respective operators and using data base query systems. Depending on the severity of the schedule deviation, these solutions are evaluated either internally (for minor deviations) or need to be coordinated at the airline's network operations center (see Fig. 1).

During the solution generation process, operators in each airline department need to correspond with external stakeholders, such as the European network management operations center (NMOC), ANSPs, ground handlers or the airport operator (Ball et al., 2007; Castro and Oliveira, 2011). While the recently introduced Airport operations center (APOC) aims at improving communication processes between stakeholders, the actual decision-making about which recovery actions to take for a disturbed flight schedule remains entirely with the AOCC (Eurocontrol, 2018). Thereby, several research projects have identified the current AOCC procedures to be antiquated and inefficient, considering that a department-specific solution generation is highly iterative and delivers at best only sub-optimal solutions. Despite the aim for a (partial) automation and integration of AOCC decision-making described in many studies, only few have accomplished to incorporate multiple airline network layers (departments) at once into the solution finding process. Most frequently, methods are proposed for a joint optimization of aircraft recovery (usually done in the airline's network operations center) and passenger and/or crew recovery (Bratu and Barnhart, 2006; Clausen et al., 2010; Eggenberg et al., 2010; Petersen et al., 2012b; Dunbar et al., 2014; Hu et al., 2016; Vink et al., 2020), while only few consider specific maintenance constraints (Liang et al., 2018) or allow flexibility in flight planning (e.g., dynamic cost-indexing as in Delgado et al. (2016), Marla et al. (2017), Arikan et al. (2016)). Notably, all modelling approaches entirely neglect the AOCC ground operations control unit and the related recovery potential during the turnaround. Merely two models implement aspects of ground operations by assigning additional costs for an accelerated turnaround (Stojković et al., 2002) and constrained aircraft parking positions per airline (Santos et al., 2017). In contrast, most studies which focus on airline ground operations and airport logistics miss a relation to AOCC decision-making.

### 1.2. Focus and structure

We present an optimization approach which integrates turnaround recovery, i.e., the consideration of alternative procedures and resource allocations during ground operations as a way to recover the effects of schedule deviations or disturbances, into existing solutions for integrated aircraft, crew and passenger recovery, while respecting maintenance constraints. We aim to fill the scientific gap on AOCC decision support across multiple departments by incorporating the largest contributor to airline delay, i.e., the turnaround.

Our approach combines an aircraft routing model with a resource-constrained turnaround scheduling model to predict delay propagation within an airline hub network. Combining both models allows us to introduce different recovery options which can adapt and rebuild the initial flight schedule in addition to existing schedule buffers (1) locally at the airport during the turnaround; (2) network-wide in the context of downstream dependencies for aircraft, crew and passengers; and (3) integrated during turnaround and/or downstream operations. In order to demonstrate the feasibility of our concept, we implement all models (individual and integrated) into a dynamic optimization algorithm with rolling horizon and apply them in the context of a case study. Therein, the network resilience of an exemplary airline with hub at Frankfurt airport is studied and we compare the recovery performance of the integrated model with the performance of the individual aircraft and turnaround models under the influence of primary delays during the morning hub bank (which might spill over into the afternoon and evening hub banks).

The article is structured into six sections. Section 2 presents a detailed literature review on delay propagation and the context of airline schedule planning, schedule recovery and ground operations. Section 3 describes the used methodology to integrate turnaround and aircraft recovery. In Section 4, the case study setting and scenario framework is introduced in which the models are applied. Section 5 highlights the results of the scenario analysis. Finally, Section 6 discusses the results from previous sections, provides conclusions and emphasizes future work aspects.

## 2. Literature review

As highlighted before, robust airline schedule planning, schedule recovery and ground operations have been treated as separate research topics in the past. While the impact of delay propagation is incorporated in strategic schedule planning approaches by using historical operations data, it is mostly neglected in the latter two problems. At best, schedule recovery models use statistically fitted delay multipliers instead of focusing on case-specific interdependencies, whereas models on ground operations rarely consider any delay impact outside the airport system. This sections details the advancements in each area of research to derive the current state-of-the-art.

### 2.1. Robust schedule planning

Robust schedule planning is a proactive strategy that aims at designing flight, crew and passenger schedules "robust" in advance, such that delays have no or only a few negative consequences on downstream interdependencies. Robust scheduling approaches typically include the provision of reserve resources (aircraft or crews), the paired routing of aircraft and crews within so-called short-cycles (Rosenberger et al., 2004) as well as block (Sohoni et al., 2011) and ground time buffers (Aloulou et al., 2010; Gupta et al., 2018). Furthermore, some studies reallocate available buffer times by adapting the departure times of sensitive flights (AhmadBeygi et al., 2010b; Wu, 2006), whereas other approaches consider the possibility of in-flight acceleration (variable block times) during flight schedule design (Safak et al., 2017; Sinclair et al., 2016a). In addition to buffer times, stochastic disturbance data are used to identify critical links in a scheduled

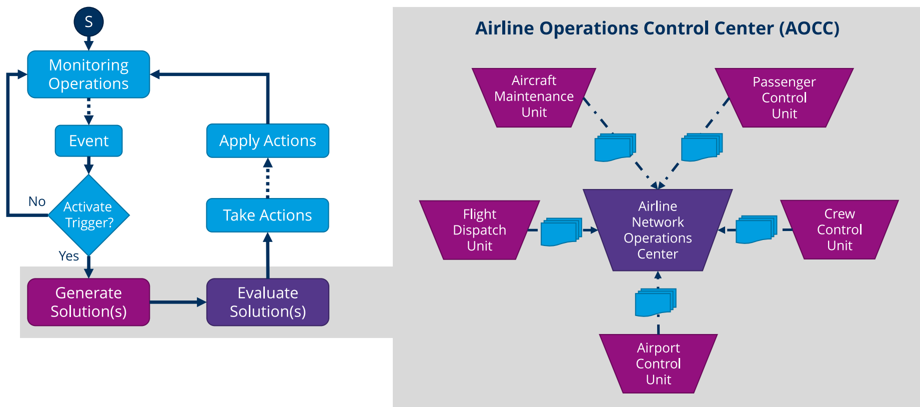


**Fig. 1.** Control loop and department-hierarchy within a typical Airline Operations Control Center (AOCC).

aircraft routing to reduce the propagation of delay (Yan and Kung, 2018; Wu and Law, 2019).

Despite the efforts undertaken by proactive planning, schedule disruptions are inevitable given that not all disturbances are predictable and controllable at the strategic planning level for an entire season in advance. For this reason, reactive strategies, such as schedule recovery, are required at the tactical level (i.e., around the day of operations) to enable a fast and cost-effective adaptation of the schedule to recover the performance of the airline network.

### 2.2. Schedule recovery

As initially mentioned, the schedule recovery process takes place in the AOCC and is sub-divided according to different airline departments, which each focus on the impact of a schedule deviation on their particular network layers, such as aircraft routings, crew rosters or passenger itineraries. Consequently, many early optimization approaches in the field of airline schedule recovery have only considered the problem of a specific department, whereas just recently and with the advancement of computational capacities, there have been more proposals on how to model integrated schedule recovery. In the case of department-specific recovery approaches, it needs to be considered that a typical hierarchy was adopted from the solution-finding procedures in the AOCC, such that aircraft schedules are recovered first, crews rosters second and passenger itineraries at last, given that passengers cannot fly without the prior two being feasible and available (Kohl et al., 2007; Clausen et al., 2010).

#### 2.2.1. Aircraft recovery

A comprehensive overview on modelling approaches for aircraft recovery can be found in Clausen et al. (2010). Thus, applied problem classes include network flow problems and set partitioning problems. The difference between them is that the prior typically aims at finding cost-minimal routings which cover the entire trajectory of an aircraft, including several flight, ground and maintenance arcs (Yan and Yang, 1996; Eggenberg et al., 2010; Liang et al., 2018), whereas the second assigns flights individually either to sets of pre-defined aircraft routings or to a set of cancellations (Rosenberger et al., 2003; Andersson and Värbrand, 2004; Clausen et al., 2010). Among the network flow models, some simplified approaches do not consider specific arcs for maintenance or ground processes (Bard et al., 2001), whereas others introduce additional so-called *protection arcs* to minimize the deviation from the original flight schedule (Thengvall et al., 2000) or put additional constraints to adhere to airport slots (Liang et al., 2018). Among all, the key recovery measure to restore the schedule are aircraft swaps or equipment changes — whereby the prior swaps the flight assignment between two aircraft of the same fleet, whereas in the latter case, another aircraft type is assigned to a flight. Atkinson et al. (2016) find delay-reducing effects when airlines schedule more aircraft of the same type to take off and land at the same airport within a similar time frame, such as a hub bank, given the increased flexibility for aircraft swaps. Conversely, cross-fleet equipment changes are applied in Løve et al. (2002), Xu et al. (2019), Lonzius and Lange (2017).

#### 2.2.2. Crew recovery

The problem of crew recovery is similar to that of *aircraft swaps*, except that legislation imposes much more complex duty time regulations for the affected personnel. Furthermore, crew pairings do not always align with aircraft rotations, such that crew transfer between aircraft impose further network interdependencies over the entire day of operations. There are three different approaches to this issue in the literature, such that: (1) the aircraft schedule is regarded as fixed and cannot be changed due to its higher rank in the recovery hierarchy (Medard and Sawhney, 2007); (2) some flights might be cancelled if no efficient crewing solution can be found (Lettovský et al., 2000); or 3) delays might be assigned to some flights to find a feasible crew assignment (Abdelghany et al., 2004; Stojkovic and Soumis, 2005; Clausen et al., 2010). Given the nature of the problem, such that multiple crew members need to be assigned to all flights, all studies define either multi-commodity flow networks (Stojkovic and Soumis, 2005) or set covering problems (Medard and Sawhney, 2007; Lettovský et al., 2000), while proposed solution algorithms include large neighbourhood heuristics (Sinclair et al., 2014) or column generation heuristics (Medard and Sawhney, 2007; Stojkovic and Soumis, 2005; Sinclair et al., 2016b).

#### 2.2.3. Integration of aircraft and crew recovery

Abdelghany et al. (2008) extend their initial crew recovery model (Abdelghany et al., 2004) to cover multiple resource types, i.e., aircraft and crews. This is done with an integration of a schedule simulation and a resource optimization model within a rolling horizon framework. Zhang et al. (2015) propose a two-stage heuristic algorithm for the integrated aircraft and crew recovery problem. Thereby, separate multi-commodity flow networks are optimized iteratively for each resource type while considering a simplified version of the other flow network. Maher (2016) argues that set partitioning and Benders' decomposition approaches as proposed in Lettovsky (1997) and Petersen et al. (2012b) do not guarantee integer optimal solutions and presents a column-and-row generation as part of a branch-and-price algorithm for his integrated aircraft and crew recovery model.

#### 2.2.4. Integrated approaches including passenger recovery

It has only been in recent years, that passenger recovery has received increasing attention and has been studied independently of aircraft and crew recovery. Two separate studies have analysed trade-offs between in-flight acceleration to reduce inbound delays and outbound delays at the gate, such that passengers transfer connections are maintained at hub airports (Delgado et al., 2016; Mazzarisi et al., 2019; Marla et al., 2017). Arikan et al. (2016) also incorporate cruise speed control when they integrate aircraft and passenger recovery with a mixed-integer non-linear problem (MINLP). Next to flexible fuel burn, Santos et al. (2017) consider airport capacity constraints, such as limited parking positions, taxiway capacity and runways slots, whereby they assume that the airlines can alter the sequence of their arrival and departure flights within all their runway slots to guarantee passenger's minimum connection time. Furthermore, they assume a rolling horizon to break down the recovery problem into smaller periods, which are then feasible for the solution with mixed-integer linear programming. Hu et al. (2016) solve their set partitioning problem for integrated aircraft and passenger recovery with the GRASP algorithm and a passenger reassignment algorithm. In an early work, Bratu and Barnhart integrate aircraft flight scheduling with passenger and crew constraints (Bratu and Barnhart, 2006). Thus, they are among the first to jointly consider passenger delay costs and airline operating costs in the same objective function. Cook and Tanner (2015) later highlight that passenger delay costs to airlines are substantially different to flight delay costs, given that passenger arrival delays are higher on re-booked itineraries and may require extensive compensation payments. Given that passengers are not part of the airline and have different objectives, Yang and Hu (2019) propose a bi-objective model which aims at minimizing the additional costs for the airline and the utility-loss for passengers. The problem is solved by using a multi-criteria genetic algorithm.

Integrated modelling approaches for aircraft, crew and passenger recovery have been studied by Lettovsky (1997), Kohl et al. (2007) and Petersen et al. (2012a). The review of Kohl et al. (2007) concludes that the full integration considering all constraints of each problem results in extensive solution times and is unlikely to deliver a globally optimal solution, such that constraints for some sub-problems should be simplified. Petersen et al. (2012a) do exactly that by introducing simplifications to crew constraints, while the objective function targets a global optimum for aircraft and passenger recovery. Their solution algorithm includes decomposition according to Bender and column generation and was proven to be effective when less than 65% of the total flight schedule of about 800 flights are affected by a disturbance. Similar to Petersen et al. (2012a), also the study of Vink et al. (2020) uses a network flow model for each aircraft rotation which includes maintenance schedules and passenger itineraries, while crew constraints are modelled only indirectly with reserve crews being available to ensure feasibility. For the generation of real-time recovery solutions, an algorithm selects a locally available sub-set of aircraft which is then considered within the solution process.

### 2.3. Ground operations

Given that many network flow models consider the aircraft ground time in-between two flight assignments with a single *ground arc*, many interdependencies are neglected which may appear in-between aircraft during their turnaround at the same airport. Conversely, many studies which focus on airport resource interdependencies, which may arise from the allocation of parking positions (Dijk et al., 2019; Ali et al., 2019), ground handling equipment (Du et al., 2014; Padrón et al., 2016; Tomasella et al., 2019) or both at the same time (Vidosavljevic and Tosic, 2010), do so independent of airline schedule recovery. As indicated above, the model of Santos et al. (2017) is the only one that considers airport capacity constraints jointly with aircraft and passenger recovery procedures. The model of Stojković et al. (2002) is the only one to mention that turnaround times might be reduced relative to the costs for additional resources. In any other approach, the schedule recovery potential comprised in ground operations is entirely neglected, despite several studies suggesting alternative procedures for accelerated cleaning, fuelling (Kuster et al., 2009) or boarding processes (Schultz, 2018a,b). Considering that these processes typically belong to the critical path of a turnaround, the coordinated use of their recovery potential might contribute to a reduction of departure delays and, thus, make more comprehensive changes in aircraft and crew schedules obsolete.

Another limiting factor for the effective integration of ground operations into proactive and reactive airline schedule planning is that many studies still assume the turnaround of an aircraft to have a static duration. In fact, there are only a few models which acknowledge the stochastic nature of ground operations. For instance, two separate studies (Wu and Caves, 2004; Fricke and Schultz, 2009; Oreschko et al., 2012) have fitted stochastic time distributions to historical data of turnaround sub-processes with the aim of predicting target off-block times. Thereby, one approach (Fricke and Schultz, 2009; Oreschko et al., 2012) defines case-specific trigger parameters (e.g., inbound delay) which limit the data foundation used in a Monte Carlo simulation. The second study (Wu and Caves, 2004) develops a semi-Markov chain with predefined process- and delay states in which the turnaround simulation sojourns until all processes are completed. These stochastic ground times are then evaluated as potentially critical links between flights in a planned airline schedule (Wu and Law, 2019). An application within the tactical context of schedule recovery is to the best of the author's knowledge, yet to be made.

## 3. Methodology

This section introduces four mixed-integer linear programming models which are built upon an underlying flight schedule and differ from each other by the number of available recovery options. The flight schedule incorporates predefined aircraft rotations, crew pairings and passenger itineraries. Scheduled aircraft maintenance events, airport curfews and crew duty time regulations represent hard constraints to the schedule, while all flights have flexible arrival and departure time windows, outside of which an airline incurs costs of delay.

A basic Network Delay Model (NDM) is used to estimate the state of the airline network "S0" in case of deviations or disturbances when no recovery options would be available.

With the addition of aircraft, crew and passenger recovery options which can be applied throughout the entire network, the NDM is extended into an Aircraft Recovery Model (ARM) to calculate the minimum cost solution for the airline ("S1"). A separate Turnaround Recovery Model (TRM) considers only local recovery options for its solution "S2". Local means that only options are considered which can be applied to aircraft turnaround, passenger and crew transfer processes during the next bank at the airline's hub airport. The integration of both models yields an Integrated Recovery Model (IRM), which incorporates the local recovery potential at the airport as well as the network recovery potential of modified aircraft rotations in the solution process for "S3". All four models are applied to one day of network operations of an airline in a rolling horizon mode. Thereby, each period contains one hub bank of the airline schedule and solutions of previous hub banks serve as input for subsequent ones (see Fig. 2).

### 3.1. Network delay model (NDM)

The basic NDM calculates the costs of routing a set of aircraft along their predefined flight rotations. It incorporates flight plan-specific scheduling constraints (e.g.,MCT, Minimum Ground Time (MGT), Scheduled Off-Block Time (SOBT) and Scheduled In-Block Time (SIBT)), such that the integrity of the planned flight sequences per aircraft, crew pairings and passenger itineraries is maintained. The start and end times of all flights are defined by their SOBTs and SIBTs at the origin and destination airport. The period between two subsequent flights, which is required to perform all relevant ground operations, depends on the aircraft type and is referred to as the MGT. It is usually defined by the aircraft manufacturer. The MCT is a stochastic and airport-specific parameter that details the minimum time required for most passengers to reach their transfer connections via the terminal

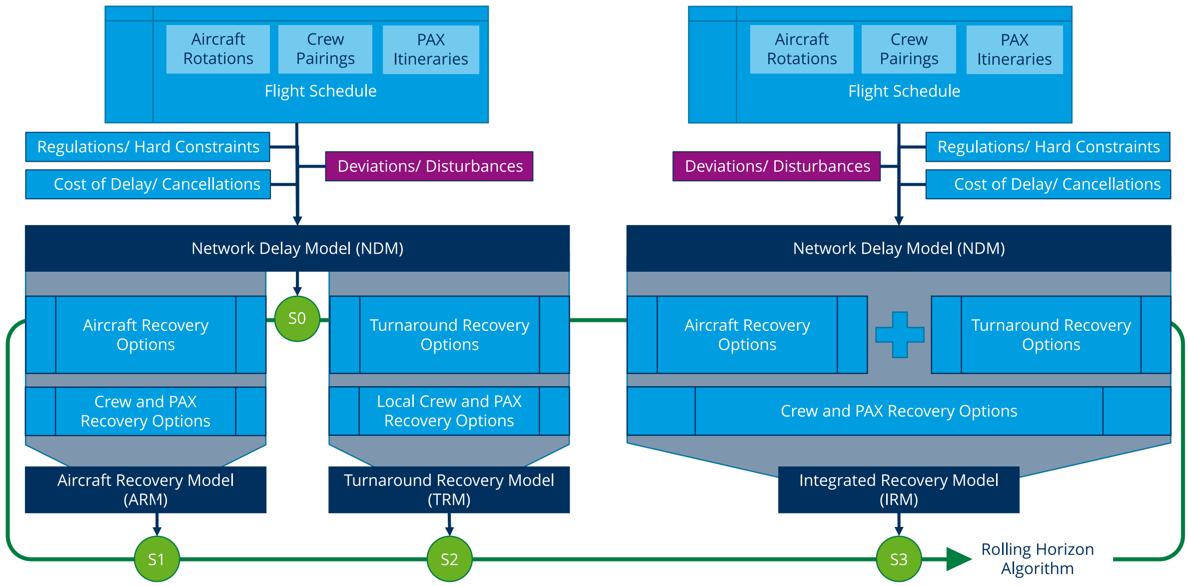


**Fig. 2.** Modelling framework of our integrated recovery approach which includes four different model instances to compare their respective solutions "S0-S3" with each other.

at the respective airport. In case of deviations from the schedule on the day of operations, the resulting delay propagates throughout the network — along the rotation of the causal aircraft, but also to other rotations which are linked to the causal aircraft by passenger or crew transfer connections. According to typical airline recovery policies, other aircraft are restricted to a maximum of ten minutes waiting time for delayed transfer passengers, before the respective passenger group is re-booked onto later flights (Schlegel, 2010a). This is to protect Air Traffic Flow Management (ATFM) slot constraints as well as to respect the cost sensitivity of deviations from the initially scheduled departure time windows. In the baseline setting, the model is primarily used to calculate the delay and cost impact resulting from a schedule deviation. This means that there is no possibility for the recovery of the flight schedule other than the rebooking of transfer passengers once the critical ten-minute threshold for departure delays is reached. Thus, the model takes a monitoring role.

### 3.1.1. *Aircraft routing*

The problem of assigning flights to individual aircraft can be abstracted as a routing between dedicated nodes (flights) with corresponding time restrictions and arcs (ground events). Appropriate for this purpose is a Vehicle Routing Problem with Time Windows (VRPTW) formulation, which generates cost-minimal tours for a set of vehicles (aircraft) and ensures that a node is only operated within a certain time window (Cordeau, 2000; El-Sherbeny, 2010). As the presented problem describes aircraft as vehicles, which all have specific operational requirements, the general VRPTW is extended to the commonly used Heterogeneous Vehicle Routing Problem with Time Windows (HVRPTW). The idea of the HVRPTW ensures that each node is visited exactly once, that each route starts and ends in an idle state, and that time window restrictions on each node as well as the individual vehicle capacities are respected. Our HVRPTW is defined by a set of unique aircraft $V$, a set of all nodes $N$ including all flights and a dummy aircraft depot 0, a set $C \subset N$ with all flights but excluding the depot and a directed graph $G = (V, C)$ (see Fig. 3). The set of ground arcs $A \subseteq N \times N$ contains all possible connections between the depot and the flights as well as in-between all flights. The costs $C^A_{ijv}$ and a minimum ground time $MGT_{ij}$ are predefined for all arcs when an aircraft $v$ transfer between flight $i$ and flight $j$ with $i \neq j$. The flight adjacency matrix $AdjF_{iv}$ restricts which flight $i$ can be served by an aircraft $v$ after each flight. $A$ can be reduced to a set of reasonable arcs $A_{red} \subseteq A$, which is also defined within the adjacency matrix, such

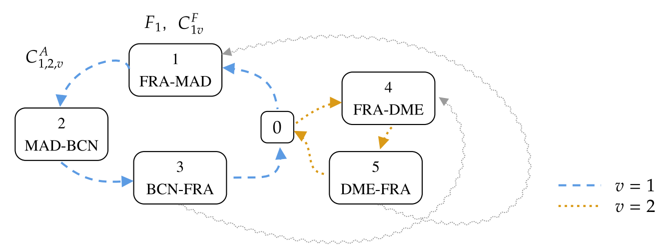


**Fig. 3.** A schematic ARP with $C = 5$ flights and two tours separated by colour ($V = 2$), which start and end at the depot ("0"). For flight 1, flight time $F_1$ and operating costs $C^F_{1v}$ and transition costs $C^A_{12v}$ are indicated for aircraft $v$. Grey arcs represent possible connections, which are not part of the illustrated minimum cost tours.

that all arcs with infeasible time constraints are omitted before the optimization. Given that the basic NDM cannot make changes to the initial aircraft-flight assignment, only the arcs from the planned flight schedule are valid.

Each flight $i$ has a given flight duration $F_i$ and aircraft-specific operating costs $C^F_{iv}$. Moreover, each flight $i$ gets a non-negative hard time window defined by the boundaries $[SOBT_i, B_i]$ which correspond to potential night curfews or ATFM capacity regulations. This means that the departure time $s_i$ and arrival time $e_i$ of the respective flight must lie within these limits. The binary decision variable $x_{ijv}$ decides whether aircraft $v$ connects between two flights $i$ and $j$ via a ground arc $(ij)$. Finally, the variable $end_v$ calculates the termination time for the entire rotation of aircraft $v$, resulting in a string of subsequent flights (see Figs. 3 and 5).

The depot represents the airline's hub, so all tours start and end at this central airport. However, depending on the configuration of the $0j$ and $i0$ in $A_{red}$, optionally other or all stations can be allowed (e.g., for night stops).

### 3.1.2. *Modelling of delay costs including passenger and crew recovery*

In addition to the hard time windows, we also introduce a set of Soft Time Windows (STW) $\Gamma$. Conversely to hard time windows, STWs tolerate a deviation from scheduled times but charge delays with costs. These costs are flight-specific and correspond to additional crew wages, maintenance expenses or a loss of passenger goodwill as described in Cook (2015), Cook and Tanner (2015). Our model considers STW only for flight delays, however, this approach may also be transferred

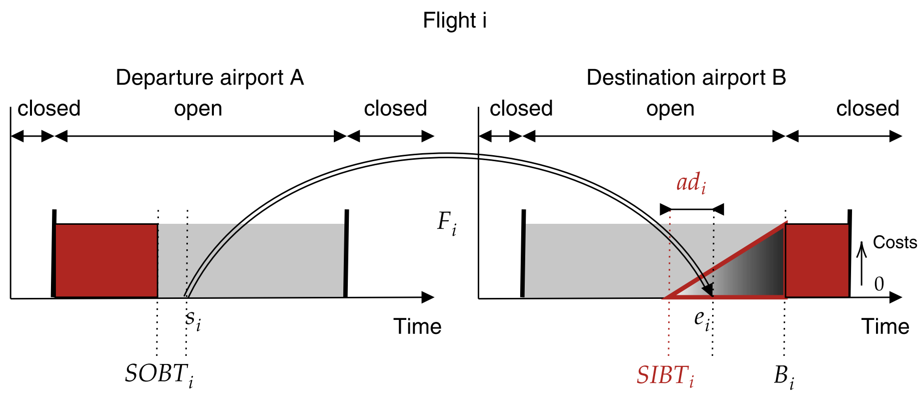


**Fig. 4.** Implementation of soft time windows for a node (flight) $i$. The grey boxes represent the airport operating times. The limits of the interval $[SOBT_i, B_i]$ for the fix time window must not hurt these restrictions for the related airport. The red triangle represents a STW, and the deviation of $e_i$ from the scheduled arrival time $SIBT_i$ is formulated as $ad_i$, which leads to increasing costs with increasing delay.

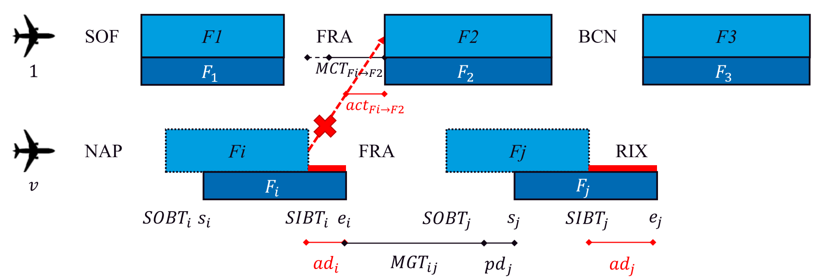


**Fig. 5.** Simplified representation of two aircraft rotations covering five flights. For aircraft $v$ the delay $ad_i$ on flight $i$ propagates and even increases towards flight $j$ because of a delay multiplier. The passenger transfer shown as a red arrow to flight F2 cannot be maintained due to the delay of flight $i$ and the MCT.

onto maintenance events if one assumes that such events can begin later than planned (which we do not because of firmly booked hangar times).

A STW $\gamma \in \Gamma$ for flight $i$ is described by the interval $[SOBT_i, SIBT_i^{\gamma}]$. A flight can have multiple STWs, such that several delay segments with marginal increasing linear costs can be described, considering that in reality, costs increase progressively with higher delay (Cook, 2015). All STWs of a flight $i$ must be within the hard time window $[SOBT_i, B_i]$. If a flight exceeds boundaries of a STW $\gamma \in \Gamma$, the arrival delay is calculated by the variable $ad_i^{\gamma}$ (positive deviation of $e_i$ from $SIBT_i^{\gamma}$ — see Fig. 4). For balancing the constraint formulations, an additional variable for arrival earliness $ae_i^{\gamma}$ represents negative deviation of $e_i$ from $SIBT_i^{\gamma}$. However, only positive deviations are part of the objective function with the corresponding arrival delay cost factor $C_i^{AD\gamma}$.

In case that a flight arrives later than scheduled and contains transfer passengers or crews for other flights, the model performs trade-offs between costs for delaying the departure (and subsequently the arrival) of these flights and the adaptation of passenger and/or crew itineraries. Therefore, we formulate airport-specific minimum connection times $MCT_{ij}$ between flights $i$ and $j$ and cancellation costs $C_{ij}^{CX}$ in case the available transfer time $act_{ij} = s_j - e_i$ is smaller than the $MCT_{ij}$. The decision about whether a transfer can be realized or needs to be cancelled is captured with binary variable $cx_{ij}$. The costs of cancelling a passenger connection depend on the available rebooking options, such that the number of passengers, the additional trip time with the next available flight towards the destination, as well as the fact that some passengers may want to abort their trip need to be considered. All these factors determine the costs for care, rebooking, reimbursement and compensation according to EU regulation 261. The cancellation of a crew connection can only be performed when a standby crew is available to step into duty, whereby the costs of this procedure are estimated as an equivalent of wage costs for extra duty time for the entire crew.

If an aircraft is delayed at departure, the delay may propagate until the end of the flight when $e_i \geq SIBT_i^{\gamma}$. In case the arrival delay infringes the MCT, the same trade-offs between waiting-for and cancelling transfer connections need to be made again at some of the downstream airports in the aircraft routing. Consequently, the costs of departure delay of each flight need to incorporate the costs of downstream flight delays or cancelled passenger connections according to the respective downstream network dependencies. Thereby, the additional costs of other flights waiting for transfer connections at the destination airport increase the slope of the costs curve, while the cancellation of connections induces sudden cost steps (see Fig. 6).

### 3.1.3. Stochastic delay propagation

Given that the necessary resources at an airport are only reserved within the initially scheduled ground time and may be needed elsewhere afterwards, there might be further disturbances impacting the turnaround of a delayed aircraft. It is the purpose of the Airport-Collaborative Decision Making (A-CDM) concept to share schedule deviations of a flight much in advance, such that the ground handling schedules can be adapted accordingly or even additional resources can be allocated to reduce the turnaround time. However, the flexibility depends on local service level agreements, the number of turnarounds an airline operates at the respective airport and the number of other airlines which are served by the respective ground handler. Based on this variable flexibility to react to potential arrival delays, we define delay multipliers $DM_i$ which are applied on the arrival delay of each flights $i$ and depend on the respective destination airport. These delay multipliers can range from values $< 1$ for airports where the airline has a lot of potentials to adapt its ground operations (i.e., typically at the hub airport or at hubs of partner airlines (Schlegel, 2010b)), whereas they are usually $> 1$ at spoke airports in the hub network (Oreschko et al., 2010). This means that arrival delays cause even higher propagated delays $pd_j$ on the next flight $j$ in the aircraft rotation. The multiplier $DM_j$ must be $\geq 0$ and may even be defined individually per flight to represent natural differences among hubs and spoke airports as well as respecting weather, day-time or traffic.

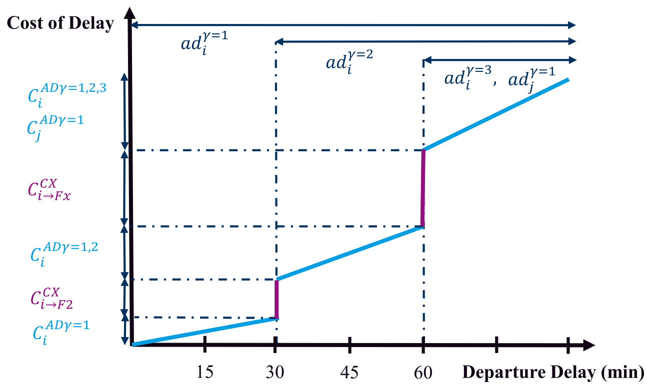


**Fig. 6.** Delay cost function for a flight including marginal time dependent costs (three STW), step-costs due to missed downstream transfer connections, and reactionary costs (stacked STWs of flights $i$ and $j$).

Fig. 5 shows the relevant variables and interdependencies schematically for the rotation of two aircraft, where the arrival delay of flight $i$ propagates with a delay multiplier $> 1$ onto flight $j$, while a passenger transfer connection towards flight $F2$ needs to be cancelled. The resulting delay cost function for flight $i$ is shown in Fig. 6 including three STW and two downstream cancellation cost steps. As departure delay increases, costs are incurred within the first STW ($\gamma = 1$) as a function of the delay time $ad_i^1$ multiplied with the cost factor $C_i^{AD1}$. At a delay of 30 min (which represents a connection buffer at downstream airports), the passenger transfer from flight $i$ towards a flight F2 is cancelled, which incurs costs according to $C_{i\to F2}^{CX}$. Afterwards, also the second STW ($\gamma = 2$) becomes active, measuring $ad_i^2$ from SIBT+30 min, such that marginal costs correspond to a value $C_i^{AD1} + C_i^{AD2}$. Starting with an arrival delay above 60 min, the third STW ($\gamma = 3$) is activated, while another passenger connection would need to be cancelled. Arrival delays exceeding 60 min on flight $i$ also propagate to flight $j$, whose first STW then becomes active and incurs reactionary delay costs.

### 3.2. Aircraft recovery model (ARM)

The NDM described in the previous Section 3.1 integrates two elements of strategic airline scheduling problems: the routing of an arbitrary aircraft and the assignment of a specific aircraft to this routing. In this section, we introduce aircraft recovery options to extend the basic NDM into an ARM, such that the aircraft assignments can be swapped or flights can be cancelled in case that schedule deviations would make the strategic schedule infeasible or inefficient to operate. Furthermore, the limitation to wait-for-passengers is lifted, such that aircraft which are receiving transfer connections can be held on position for more than ten minutes if this is more efficient for the entire network than cancelling the connection.

#### 3.2.1. Aircraft swaps

In the basic NDM, the set $A_{red}$ contains only the minimum set of arcs to reproduce the planned aircraft rotations from the initial flight schedule. In the ARM, the set $A_{red}$ is extended into $A_{ext}$ to include all arcs $(ij)$ which fulfil trivial restrictions (e.g., departure airport of flight $j$ must be equal to destination airport of flight $i$, the $SOBT_j$ must be after the $SIBT_i$ allowing the $MGT_{ij}$ and both aircraft must belong to a similar fleet). This allows swapping the initial aircraft-flight assignments, such that the routes of all aircraft can be changed as long as those flights are in the future. In this way, the propagation of the delay can be interrupted by selectively allocating time buffers after flights with high deviations.

#### 3.2.2. Flight cancellation

To allow flight cancellation, the set $V$ with its aircraft $v = 1, 2, \dots, q$ is extended by a set of virtual aircraft $\mathbb{V}$ with $v = q+1, \dots, u$, where the number of virtual aircraft $u$ is problem specific. Each virtual aircraft $v \in \mathbb{V}$ can serve any flight $i$ and is allowed to go directly from the depot to the flight and back without any detours. Since all constraints from the ARM also apply to virtual aircraft, a virtual aircraft can handle only one flight at a time and must begin and end its route in the depot, even if no flights are assigned. The operating costs $C_{iv}^F$ represent an estimation of all related costs to cancel this flight including monetary consequences (loss of passenger goodwill, compensation costs, rebooking, reimbursement). Technically, transfers related to a cancelled flight are still performed on time. Therefore, their cancellation costs must be included in $C_{iv}^F$ and need to be considered in any post-processing step. The number of aircraft in $\mathbb{V}$ must consequently be at greater equal to the number of timely overlapping cancelled flights. Otherwise, the problem is infeasible.

#### 3.2.3. Accepting delay to wait for passengers

The NDM proposes the cancellation of passenger or crew transfer connections whenever the available connecting times are smaller than the MCT (allowing only a maximum of ten minutes waiting times for departure flights). However, in some cases, the costs for rebooking passenger and crew itineraries are much higher than the estimated delay costs incurred when the departure flight would wait for more than ten minutes on these transfers. Consequently, no limitation to departure delay is applied in the ARM, such that it incorporates flight-specific trade-offs between total costs of reactionary delay and cancellation costs for the impacted connection(s). In order to do so, costs for cancelling a transfer connection $C_{ij}^{CX}$ are incorporated with their real cost values, while in the NDM they are discounted on each flight during the solution process to resemble the costs of a ten-minute departure delay. Note here that over the course of an entire season, this recovery option may interfere with the seasonal slot performance which is required to keep the flight at slot-coordinated airports according to EC regulation 95/93.

### 3.3. Turnaround recovery model (TRM)

Conversely to the ARM, which considers all flights in the airline network for the solution of schedule deviations, the TRM focuses only on those flights $i \in N_{red} \subset N$, which are part of the upcoming hub bank at the central airport. Thereby, all inbound flights $i \in N_{red}$ into the hub during this period are considered with their respective estimated arrival times $e_i$, while the model aims at minimizing the costs of propagated departure delay and schedule recovery costs across all parallel turnarounds. The previously introduced ground arcs between two flights of the same aircraft are substituted with a network of turnaround sub-processes $TP$ including all cabin and cargo servicing processes as well as fuelling (see Fig. 7). Routine maintenance checks or water and toilet servicing processes have been neglected in the model, given that they do not constitute the critical path of a nominal turnaround (Wu and Caves, 2004; Fricke and Schultz, 2009) which neglects technical malfunctions. Ground arcs between flights of different aircraft are replaced by individual passenger transfer processes $PA \subset TP$ and crew transfer processes $CR \subset TP$.

#### 3.3.1. Modelling of ground operations at Hub Airports

All process interdependencies between all flights are modelled as an extended version of the Resource-Constrained Project Scheduling Problem (RCPSP). Thus, individual turnaround sub-processes $p \in TP$ are considered as jobs and constrained airport resources as machines (shop scheduling models can be generalized as RCPSP (Nasiri, 2013)). Each aircraft requires the assignment to an airport stand $m \in CS \cup RS$, which holds the necessary equipment and personnel ready for a standard turnaround (corresponding to a typical RCPSP). Each turnaround

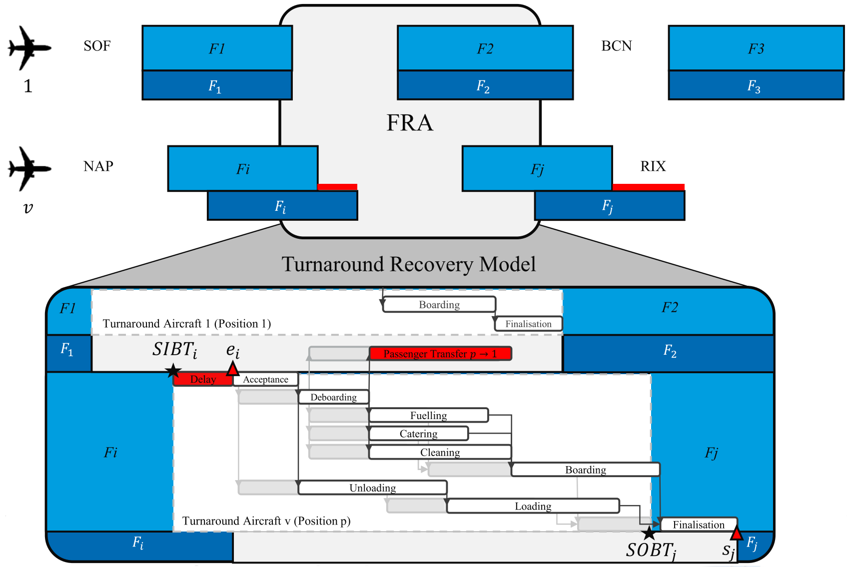


**Fig. 7.** The turnaround recovery model schedules interdependencies between turnaround sub-processes, transfer connections and resource allocations at the airline's hub airport, such that the impact of an arrival delay of aircraft $v$ can be determined and recovered at a microscopic level.

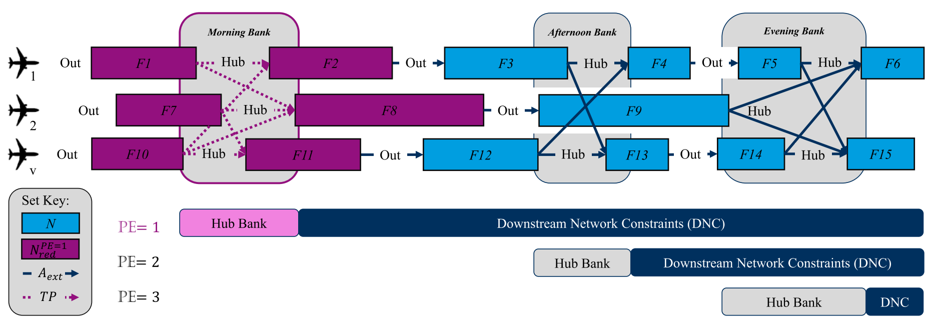


**Fig. 8.** Each period $\mathbb{PE}$ of the rolling horizon includes detailed scheduling of turnaround processes $TP$ in the next hub bank, whereby the costs of downstream flight and transfer constraints are considered for the entire day.

of an aircraft $v \in V$ is defined by a scheduled start and finishing time, which correspond to the scheduled in-block time of flight $i$ $SIBT_i$ and scheduled off-block time of flight $j$ $SOBT_j$ as introduced in the NDM. Each sub-process $p \in TP$ has a variable starting time $st_p$, a duration $D_p$, is characterized by the related aircraft $RA_p$, the related flight $RF_p$ and by links to preceding and succeeding processes determined in the turnaround adjacency matrix $AdjT_{pq} \subseteq TP \times TP$. Thereby, some processes, such as in-block $IB \subset TP$, deboarding $DE \subset TP$ or cleaning $CL \subset TP$, are related to the inbound flight, whereas other processes, such as boarding $BO \subset TP$ or finalization $FI \subset TP$, are related to the outbound flight. In-block processes $p \in IB$, which represent the first sub-process of each turnaround, can only be scheduled after the estimated in-block time $e_i$ of the related inbound flight $RF_p = i$ of the related aircraft $RA_p = v$, and once a free airport stand is available. The estimated off-block time $s_j$ as the end of the finalization process $p \in FI$ for the related outbound flight $RF_p = j$ is the result of the scheduling process. It depends on the assigned turnaround recovery decisions $\omega_v$ for aircraft $v$ as well as on recovery decisions $\kappa_p$ or $cx_p$ for passenger and crew transfer processes $p \in PA$ and $p \in CR$. Thus, the $s_j$ values which are calculated with the TRM for all outbound flights of the upcoming hub bank $j \in N_{red}$ represent the off-block times which are calculated with general $MGT_{ij}$ values for all other downstream airports.

### 3.3.2. Turnaround recovery options

Turnaround recovery options can alter the sequence of turnaround sub-processes or accelerate a sub-process by a factor $\alpha_p$, which both depends on the availability of additional airport resources (defined as extended RCPSP — (Kuster et al., 2009; Deblaere et al., 2011)). Airport resources are limited but renewable, such that they require individual sequencing. The incorporated turnaround recovery options include stand reallocation, quick-de/boarding (i.e., allocation to a remote stand to accelerate de/boarding processes) and quick-turnaround (i.e., additional staff to accelerate cleaning, catering and loading as well as parallel fuelling and boarding with fuel protection by the fire brigade). Local passenger and crew recovery decisions include quick passenger transfer (i.e., dedicated buses to accelerate the transport of transfer passenger groups to their departure gate), the cancellation of passenger transfer connections and the deployment of stand-by crews (i.e., elimination of crew transfer process if a standby crew is available) as explained in the NDM.

### 3.3.3. Departure delay and cost estimation

Aircraft occupy their allocated stands until all turnaround sub-processes are finished and, similar to the ARM, can be held on a position to maintain passenger or crew transfer connections. This may induce departure delay once the scheduled off-block time is overrun. The resulting delay incurs costs as detailed in Section 3.1.2. The costs for cancelling local passenger or crew transfer connection at the hub $C_p^{CX}$ match those introduced in the NDM. Additionally, turnaround recovery costs $C_v^{QT}$ can be related to additional ground handling fees for accelerated turnaround sub-processes, whereas a fee $C_p^{QP}$ is incurred by each quick passenger transfer service. No costs are assumed for stand reallocations.

### 3.4. Integrated schedule recovery model (IRM)

The IRM adopts all features of the ARM aside from the ground arcs between flights during the next hub bank. For the upcoming hub bank, minimum ground times $MGT_{ij}$ and minimum connecting times $MCT_{ij}$ are neglected and modelled instead with the features of the TRM:

*Sets:*

| | |
|---|---|
| $N$ | set of all flights |
| $C$ | sub set $N$ without depot |
| $N_{red}$ | sub-set of $N$, containing all inbound and outbound flights in next hub bank |
| $V$ | set of all aircraft |
| $\mathbb{V}$ | set of virtual aircraft |
| $A_{red}$ | set of all planned arcs |
| $A_{ext}$ | set of all feasible arcs |
| $\Gamma$ | set of soft time windows |
| $TP$ | sub-set of $A_{ext}$, containing all turnaround sub-processes in next hub bank |
| $IB$ | sub-set of $TP$, containing all aircraft in-block/ acceptance processes |
| $DE$ | sub-set of $TP$, containing all deboarding processes |
| $CL$ | sub-set of $TP$, containing all cleaning processes |
| $BO$ | sub-set of $TP$, containing all boarding processes |
| $FI$ | sub-set of $TP$, containing all aircraft finalization processes |
| $PA$ | sub-set of $TP$, containing all passenger transfer processes during hub bank |
| $CR$ | sub-set of $TP$, containing all crew transfer processes during hub bank |
| $CS$ | set of aircraft contact stands |
| $RS$ | set of aircraft remote stands |
| $AS$ | start and end dummy node for sequence of stand allocation |
| $QT$ | start and end dummy node for sequence of quick turnaround procedures |
| $QP$ | start and end dummy node for sequence of quick passenger transfer procedures |

*Parameters:*

| | |
|---|---|
| $C^A_{ijv}$ | costs of connecting flights $i$ and $j$ by aircraft $v$ |
| $C^F_{iv}$ | costs to serve flight $i$ by aircraft $v$ |
| $C^{AD\gamma}_i$ | cost factor if flight $i$ arrives after STW $\gamma$ ends |
| $C^{CX}_{ij}$ | costs to cancel a passenger or crew transfer |
| $C^{QT}_v$ | costs of quick turnaround option for aircraft $v$ |
| $C^{QP}_p$ | costs of quick passenger transfer for process $p$ |
| $SOBT_i, B_i$ | earliest and latest possible service times of flight $i$ |
| $SIBT^{\gamma}_i$ | end of soft time window $\gamma$ for flight $i$ |
| $F_i$ | duration of flight $i$ |
| $MGT_{ij}$ | minimum ground time between flights $i$ and $j$ |
| $MCT_{ij}$ | minimum connection time between flights $i$ and $j$ |
| $D_p$ | duration of turnaround sub-process $p$ |
| $D^{QP}$ | duration of quick passenger transfer |
| $NTT_{mn}$ | needed transfer time between stands $m$ and $n$ |
| $TT$ | transition time between airport stands |
| $DM_i$ | delay multiplier on flight $i$ |
| $\alpha_p$ | time reduction factor for sub-process $p$ |
| $QTR$ | number of available quick turnaround resources |
| $QPT$ | number of available quick passenger transfer buses |
| $AdjF_{iv}$ | adjacency matrix for aircraft-flight assignment |
| $AdjT_{pq}$ | adjacency between turnaround sub-processes $p$ to $q$ |
| $RA_p$ | related aircraft to turnaround sub-process $p$ |
| $RF_p$ | related flight to turnaround sub-process $p$ |
| $M$ | context-specific big M |

*Variables:*

| | |
|---|---|
| $x_{ijv}$ | binary variable, 1 if flights $i$ and $j$ are served by aircraft $v$ |
| $s_i$ | start time to serve flight $i$ |
| $e_i$ | end time to serve flight $i$ |
| $end_v$ | end time of aircraft rotation |
| $pd_j$ | propagated delay of flight $j$ |
| $ae^{\gamma}_i$ | estimated arrival time before STW $\gamma$ of flight $i$ closes |
| $ad^{\gamma}_i$ | estimated arrival time after STW $\gamma$ of flight $i$ closes |
| $cx_{ij}$ | binary variable, 1 if transfer from flight $i$ to $j$ is cancelled |
| $st_p$ | starting time of turnaround sub-process $p$ |
| $\omega_v$ | binary variable — equal to 1 if quick turnaround option is applied to aircraft $v$, and 0 otherwise |
| $\kappa_p$ | binary variable — equal to 1 if quick transfer option is applied to transfer process $p$, and 0 otherwise |
| $\chi_{vm}$ | binary variable — equal to 1 if aircraft $v$ is assigned to stand $m$, and 0 otherwise |
| $xT_{vw}$ | binary variable for determining the sequence of quick turnaround procedures over all aircraft $v, w \in V$ beginning and ending at an dummy node $QT$ |
| $xP_{pq}$ | binary variable for determining the sequence of quick passenger transfer procedures over all transfer processes $p \in PA$ beginning and ending at dummy node $QP$ |
| $xS_{vwm}$ | binary variable for determining the sequence of all aircraft $v, w \in V$ on stand $m \in CS \cup RS$ beginning and ending at dummy node $AS$ |

$$\min \sum_{v\in V\cup\mathbb{V}} \sum_{(ij)\in A_{ext}} C^A_{ijv}\, x_{ijv} + \sum_{v\in V\cup\mathbb{V}} \sum_{(ij)\in A_{ext}, i\geq 1} C^F_{iv}\, x_{ijv} + \sum_{i\in C}\sum_{\gamma\in\Gamma} C^{AD\gamma}_i\, ad^{\gamma}_i$$
$$\sum_{v\in V} C^{QT}_v\, \omega_v + \sum_{p\in PA\cup CR} \left( C^{QP}_p\, \kappa_p + C^{CX}_p\, cx_p \right) + \sum_{(ij)\in A_{ext}\setminus TP} C^{CX}_{ij}\, cx_{ij} \tag{1}$$

$$\text{s.t.} \quad \sum_{v\in V\cup\mathbb{V}} \sum_{i\in N,(ij)\in A_{ext}} x_{ijv} = 1 \qquad \forall j \in C \tag{2}$$

$$\sum_{(0j)\in A_{ext}} x_{0jv} \leq 1 \qquad \forall v \in V\cup\mathbb{V} \tag{3}$$

$$x_{ijv} = 0 \qquad \forall (ij) \in A_{ext}; \forall v \in V \cup \mathbb{V} \mid AdjF_{iv} = 0 \tag{4}$$

$$\sum_{i \in N} x_{imv} - \sum_{j \in N} x_{mjv} = 0 \qquad \forall m \in C; \forall v \in V \cup \mathbb{V} \tag{5}$$

$$SOBT_i \leq s_i \leq B_i \qquad \forall i \in N \tag{6}$$

$$SOBT_i \leq e_i \leq B_i \qquad \forall i \in N \tag{7}$$

$$e_j - end_k + M\,(1 - x_{0jv}) \geq F_j + pd_j + MGT_{0j} \qquad \forall (0j) \in A_{ext}, \forall v \in V \cup \mathbb{V} \tag{8}$$

$$e_j - e_i + M\,(1 - x_{ijv}) \geq F_j + pd_j + MGT_{ij} \qquad \forall (ij) \in A_{ext} \backslash TP, i \geq 1, j \geq 1, \forall v \in V \cup \mathbb{V} \tag{9}$$

$$s_i + F_i = e_i \qquad \forall i \in N, i \geq 1 \tag{10}$$

$$e_i = SIBT_i^{\gamma} + ae_i^{\gamma} - ad_i^{\gamma} \qquad \forall i \in N, i \geq 1; \forall \gamma \in \Gamma \tag{11}$$

$$s_j - e_i + M\, cx_{ij} \geq MCT_{ij} \qquad \forall (ij) \in A_{ext} \tag{12}$$

$$pd_j + M\,(1 - x_{ijv}) \geq (DM_j - 1)\, ad_i^1 \qquad \forall (ij) \in A_{ext}; \forall v \in V \cup \mathbb{V} \tag{13}$$

The objective function (1) minimizes the operating and delay costs of all flights, the costs of cancelling flights, passenger or crew connections as well as the costs of assigning turnaround recovery options during the next hub bank. Constraints (2) ensure that each flight is assigned with exactly one aircraft, even if this may be by a virtual aircraft. Constraints (3) specify that an aircraft can only perform one tour while constraints (4) restrict impossible assignments. The usual flow balance constraints of a VRPTW are described by (5). According to (6)–(7), the beginning of a flight cannot be earlier than the scheduled off-block time and must not start or end later than the curfews at origin and destination airports. MTZ sub tour elimination constraints (8) and (9) build a feasible sequence of flights for each aircraft starting at the depot. Constraints (10) are required to calculate the end times of each flight. Constraints (11) calculate the deviation from any STW. The decision if a passenger or crew transfer must be cancelled is formulated by constraints (12). Finally, constraints (13) calculate the resulting delays by applying a delay multiplier to a preceding arrival delay.

All constraints listed above are also valid for the ARM, while the NDM does not comprise the set of virtual aircraft $\mathbb{V}$ and has less feasible arcs by using the set $A_{red}$ instead of $A_{ext}$ such that aircraft cannot be swapped. On the other side, the IRM integrates all listed constraints with detailed scheduling constraints for the turnaround at the next hub airport which are presented below:

$$st_p \geq e_i \qquad \forall p \in IB \mid RF_p = i; \forall i \in N_{red} \tag{14}$$

$$st_p + D_p \leq SOBT_j + s_j \qquad \forall p \in FI \mid RF_p = j; \forall j \in N_{red} \tag{15}$$

$$st_q \geq st_p + D_p \qquad \forall p \in IB; \forall q \in TP \mid AdjT_{pq} = 1 \tag{16}$$

$$st_q \geq st_p + D_p\,(1 - \chi_{vm}) + \alpha\, D_p\, \chi_{vm} \qquad \forall p \in DE \cup BO; \forall q \in TP \mid AdjT_{pq} = 1; RA_p = v; \forall m \in RS \tag{17}$$

$$st_q \geq st_p + NTT_{mn}\, \chi_{vm}\, \chi_{wn} - M\left(\kappa_p + cx_p\right) \qquad \forall p \in PA \cup CR; \forall q \in BO \mid AdjT_{pq} = 1; RA_p = v,\ RA_q = w; \forall m, n \in CS \cup RS \tag{18}$$

$$\sum_{m \in CS \cup RS} \chi_{vm} = 1 \qquad \forall v \in V \tag{19}$$

$$\sum_{v \in V \cup AS} xS_{vwm} = \chi_{vm} \qquad \forall w \in V; \forall m \in CS \cup RS \tag{20}$$

$$\sum_{w \in V \cup AS} xS_{vwm} = \chi_{vm} \qquad \forall v \in V; \forall m \in CS \cup RS \tag{21}$$

$$st_q \geq st_p + D_p + TT - M\,(1 - xS_{vwm}) \qquad \forall v \in V; \forall w \in V \cup AS; \forall m \in CS \cup RS; \forall p \in FI \mid RA_p = v; \forall q \in IB \mid RA_q = w \tag{22}$$

Thereby, the start of each turnaround during the next hub bank can only be scheduled after the respective estimated in-block time (14). If the calculated off-block time overruns the SOBT, departure delay is assigned to the outbound flight (15). Standard RCPSP constraints (16) ensure that all turnaround sub-processes which succeed the aircraft acceptance process can only start after its completion. Constraints (17) consider reduced de-/boarding duration for all aircraft that are assigned to a remote stand. Constraints (18) determine needed transfer times for passenger and crew connections based on the stand allocation of the inbound and outbound aircraft, whereby these constraints are neglected once quick passenger transfer services are assigned or the connection is cancelled. Note that these constraints are quadratic and should be linearized for the solution with standard solvers (as shown in Evler et al. (2021a)). According to constraints (19), each aircraft has to be assigned to exactly one stand, whereby the MTZ-formulation in constraints (20)–(22) ensures that not more than one aircraft is assigned to one stand at a time. The extended RCPSP version comprises further constraints which comprise variable sub-process durations and depend on the assignment of extra ground handling resources:

$$st_q \geq st_p + D_p\,(1 - \omega_v) + \alpha\, D_p\, \omega_v \qquad \forall p \in CL; \forall q \in TP \mid AdjT_{pq} = 1, RA_p = v \tag{23}$$

$$\sum_{v \in \{V \cup QT\}} xT_{vw} = \omega_w \qquad \forall w \in V \tag{24}$$

$$\sum_{w \in \{V \cup QT\}} xT_{vw} = \omega_v \qquad \forall v \in V \tag{25}$$

$$st_q \geq st_p + TT - M\,(1 - xT_{vw}) \qquad \forall v \in V; \forall w \in V \cup QT; \forall p, q \in AC \mid RA_p = v, RA_q = w \tag{26}$$

$$\sum_{v \in QT} xT_{vw} \leq QTR \qquad \forall w \in V \tag{27}$$

$$st_q \geq st_p + D^{QP} - M\,(1 - \kappa_p) \qquad \forall p \in PA; \forall q \in BO \mid AdjT_{pq} = 1 \tag{28}$$

$$\sum_{p \in PA \cup QP} xP_{pq} = \kappa_q \qquad \forall q \in PA \tag{29}$$

$$\sum_{q \in PA \cup QP} xP_{pq} = \kappa_p \qquad \forall p \in PA \tag{30}$$

$$s_q \geq st_p + d^{QP} + TT - M\,(1 - xP_{pq}) \qquad \forall p \in PA; \forall q \in PA \cup QP \tag{31}$$

$$\sum_{p \in QP} xP_{pq} \leq QPT \qquad \forall q \in PA \tag{32}$$

$$\kappa_i + cx_i \leq 1 \qquad \forall p \in PA \tag{33}$$

Constraints (23) and (28) show exemplary for cleaning and passenger transfer, how sub-processes can be accelerated by the application of recovery options. Thereby, further MTZ-formulations are required to ensure that the limited number of turnaround resources (27) is assigned to only one turnaround at a time (24)–(26). Likewise, constraints (29)–(31) build a sequence between quick passenger transfer services. The number of parallel sequences is limited by (32), while (33) considers that a passenger connection is either assigned with a quick transfer service or cancelled.

### 3.5. Rolling horizon algorithm

All four models are implemented into a dynamic optimization algorithm that operates with a rolling horizon. For the rolling horizon, the entire day of operations is split into several periods $\mathbb{PE}$ which each contain detailed scheduling constraints for the next upcoming hub bank and aircraft routing constraints for the rest of the day. Each aircraft can only visit the hub once per period, such that the shortest hub cycle (i.e., the period from departure at hub until the arrival from spoke-airport) is the determining factor for the length of all periods (see Fig. 8).

Within each period $pe \in \mathbb{PE}$, the algorithm identifies all inbound and outbound flights which belong to the next hub bank and includes them into the sub-set $N_{red}$. Afterwards, the ground arcs between all flights which are part of the hub bank are omitted from $A_{ext}$ and included into $TP$. With this configuration, each model optimizes a given schedule deviation. As a result, the arrival times of all flights out of the hub bank are calculated according to the assigned optimal departure delays and the aircraft flight assignment is updated as described in Algorithm 1.

**Algorithm 1:** Rolling Horizon Algorithm

**Input** : $e_i$, $F_i$, $SOBT_j$, $N$, $V$, $A_{ext}$, $x_{ijv}$, $\mathbb{PE}$
**Output**: $s_j$, Updated $e_j$, Optimal Tail Assignment $\mathbb{X}_{ijv}$
**for** $pe \leftarrow 1$ **to** $\mathbb{PE}$ **do**
  **for** $i, j \leftarrow 1$ **to** $N$ **do**
    $N_{red} \leftarrow$ include all flights $i, j$ which belong to next hub bank
    **for** $(ij) \leftarrow 1$ **to** $A_{ext}$ **do**
      $A_{ext} \leftarrow$ omit all ground arcs $(ij)$ between flights of $N_{red}$
      $TP \leftarrow$ include all ground arcs $(ij)$ between flights of $N_{red}$
  Run NDM/ARM/TRM or IRM
  **for** $j \leftarrow 1$ **to** $N_{red}$ **do**
    **forall the** *elements of* $e_j$ **do**
      **if** $s_j > SOBT_j$ **then**
        $e_j \leftarrow$ update parameter $e_j = s_j + F_j$
  **for** $i, j \leftarrow 1$ **to** $N$ **do**
    **for** $v \leftarrow 1$ **to** $V$ **do**
      **forall the** *elements of* $\mathbb{X}_{ijv}$ **do**
        **if** $\mathbb{X}_{ijv} \neq x_{ijv}$ **then**
          $\mathbb{X}_{ijv} \leftarrow$ update tail assignment for next iteration $pe + 1$ (only in ARM/IRM)

## 4. Implementation

The outlined methodology is applied to a case study of an exemplary airline that operates a hub network out of Frankfurt Airport (FRA). To adopt realistic schedule conditions, flight plan data have been retrieved from the summer schedule 2019 of a local hub carrier. This section details the scope of the case study, along with the parameter setting and the introduced delay scenarios.

### *4.1. Case study setting*

The airline network of our case study includes 17 aircraft (four wide-body aircraft and 13 narrow-body aircraft), which are scheduled to operate 85 flights from and to the central hub at Frankfurt airport. One aircraft has a scheduled maintenance ("MRO") event at FRA in the afternoon. Ten long-haul intercontinental flights are assigned to the fleet of long-haul aircraft (i.e., Boeing B748), whereas the remaining 75 flights are distributed among a fleet of Airbus A320 and A321 aircraft. The majority of aircraft meet during three hub banks throughout the day, which includes a morning hub bank from 5:30 a.m. to 9:00 a.m. UTC, an afternoon hub bank from 12:00 p.m. to 3:30 p.m. UTC and an evening hub bank from 5:00 p.m. to 8:30 p.m. UTC (see Fig. 9). The length of all hub banks is defined such that each aircraft can only visit the hub once during each bank, which creates the need for another "midday hub bank", where two aircraft meet between 10 a.m. and 12 a.m. UTC. However, given the limited interdependencies between these two aircraft, this hub bank is not further considered in the case study.

### *4.2. Parameter definition*

#### *4.2.1. Passenger itineraries and crew pairings*

Passenger transfer connections are simulated for the entire day between all feasible flight pairs, such that they respect the minimum connecting time at FRA (i.e., 45 min) and avoid extreme detours (e.g., passengers from Madrid are unlikely to connect via FRA to Barcelona). Thereby, a typical average load factor of a network carrier (i.e., 85%) and the reported connection ratio at FRA are considered (i.e., 55%). While all passenger itineraries include a maximum of two flight legs, passengers who originate in FRA may have transfer connections at spoke airports in the network, which are themselves a hub airport to a partner airline (these airports are marked in orange in Fig. 9).

As described above, the costs of cancelling a passenger transfer connection $C_{ij}^{CX}$ depend on the available rebooking alternatives, which again depend on the frequency of the respective route and remaining capacities on the respective flights. Thus, a baseline administrative charge and reference delay cost values per impacted passenger are adopted from Cook and Tanner (2015) such that they consider the arrival delay at destination and the corresponding costs for care, reimbursement, compensation and lodging according to EU regulation 261.

Crew pairings have been determined in accordance with official duty time regulations and contain several aircraft changes at FRA. The cancellation of crew transfers requires the availability of a stand-by crew (of which there is one positioned for continental flights during each hub bank) and incurs cancellation costs ($C_{ij}^{CX} = 1000$) similar to the wage for two extra working hours of the entire crew (Cook et al., 2009).

#### *4.2.2. Initial stand allocation during hub bank*

The initial stand allocation for each hub bank considers the number of transfer passengers on all connections and adheres to official operational constraints. Thus, contact stands at Terminal 1 A (Stands A1-2 and A4-5 in Fig. 10) are reserved for flights to and from Schengen countries only. Contact stands with special security and customs areas (Stands A3, A6, B1 and C1) can also operate flights to and from Non-Schengen destinations. Thereby, stands A3 and A6 are predominantly used for intercontinental flights with wide-body aircraft. Remote stands R1 and R2 are located on the apron, such that passengers need to be transferred with buses via the central bus station (marked with a bus icon in Fig. 10). During the morning and evening hub bank, all wide-bodies, as well as flights from and to Tel-Aviv (TLV), are fixed at their initial stands, whereas the remaining aircraft can be re-allocated to any other stand which complies with the security procedures of the respective origin and destination countries.

#### *4.2.3. Turnaround process times and cost values*

Airport service times ($A_i$, $B_i$) and minimum transfer times ($MCT_{ij}$) outside of the hub are considered as publicly disclaimed on the respective websites, such that we consider a night curfew at FRA which lasts from 11 p.m. to 5 a.m., whereas further night curfews are incorporated for many major European airports. Flight durations ($F_i$) are adopted from the flight plan as well as buffer times during the turnaround or via transfer connections. If not modelled explicitly by the TRM, minimum ground times ($t_{ij}$) correspond to those values published by the aircraft manufacturer. For the upcoming hub bank, the TRM estimates the duration of individual turnaround sub-processes ($D_p$) by

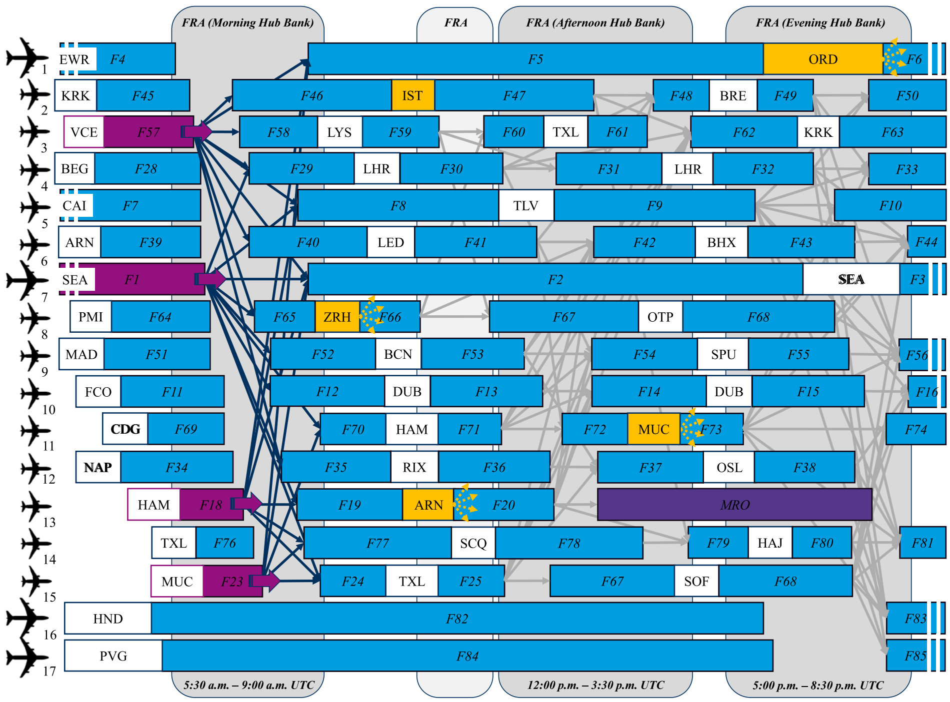


**Fig. 9.** Airline network for one day of operations, which includes the routing of 17 aircraft between three major hub banks in Frankfurt (morning, afternoon, evening). From interdependencies within each hub bank, it is visible that a delay scenario including four arrival flights of the morning hub bank may impact almost the entire downstream flight schedule. Spoke airports marked in orange are hub airports of partner airlines and contain further passenger transfer connections.

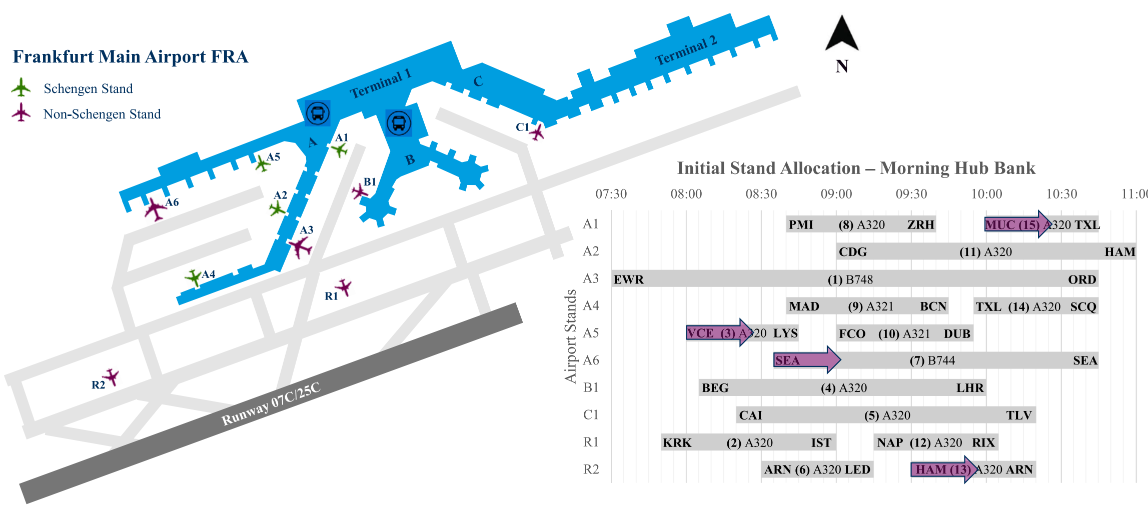


**Fig. 10.** Case study setting at Frankfurt Airport (FRA) with initial stand allocation during the morning hub bank. Aircraft turnarounds which are impacted by arrival delays as part of the scenarios are marked by magenta arrows.

considering the 80%-quantile of fitted probability density functions as described in Fricke and Schultz (2009), Oreschko et al. (2012). Once additional airport resources and personnel are assigned to operate a quick turnaround, the time factor $\alpha_p = 0.7$ is applied to the controlled sub-processes. The procedure is limited to a maximum of one parallel quick-turnaround ($QTR = 1$) and incurs a charge per turnaround ($C_v^{TR} = 300$) which was adopted from an undisclosed service level agreement of a ground handler. The same time factor $\alpha_p$ applies to deboarding and boarding processes once an aircraft is allocated to a remote stand. However, there is no charge for changing the stand allocation, as airlines typically have long-term agreements at their hub airports which reserve them the unrestricted usage of specific stands. Furthermore, there is one dedicated bus that can operate quick transfer services ($QPT = 1$) for a fixed charge ($C_v^{TR} = 100$) per assignment.

Direct operating costs $C_{iv}^F$ to serve a flight are simplified and assumed to be distance-dependent, where the great circle distance is multiplied by a cost factor for each fleet. However, the initial assignment of aircraft to flights of the adopted flight plan is induced by a significant cost reduction, such that arbitrary aircraft swaps are mitigated.

Aircraft-specific arrival delay costs $CAD_i^\gamma$ are considered per minute and include additional crew wages, maintenance expenses and costs of passenger dissatisfaction according to the size of the respective aircraft as described in Cook (2015), Cook and Tanner (2015). Thereby, the end of the first STW ($\varphi_i^1$) corresponds to the scheduled in-block time (SIBT), whereas the second STW does not include any costs for deviations of less than 15 min. A third STW ranges until arrival delays of 30 min, such that marginal costs of delay are increasing from each of these

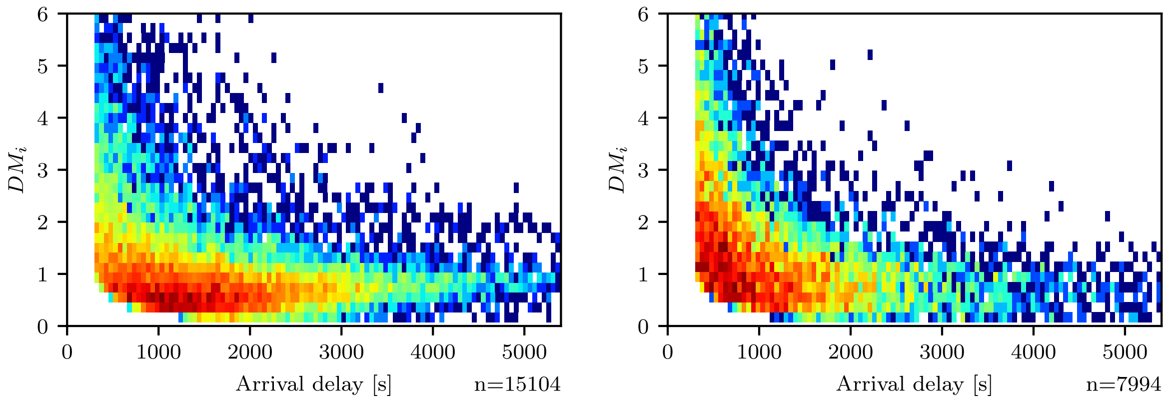


(a) Hub FRA (b) Other Non-Alliance Hubs

**Fig. 11.** The heat map exhibits the frequency (from blue to red) that a given arrival delay has multiplied with the respective $DM$. The 2D histogram is limited to flights within the network of a German hub carrier which obtained arrivals delays between 5 and 90 min during the summer season of 2019. Airport- and airline-specific delay multiplier $DM_i$ depending on arrival delay of flight $i$.

**Table 1**
Four arrival flights of the morning hub bank (F1, F18, F23, F57) obtain different arrival delays in each scenario, such that the recovery performance of all models (ARM, TRM, IRM) can be compared when the network faces schedule deviations in different magnitudes.

| Scenario ID | Arrival Delay F1 | Arrival Delay F18 | Arrival Delay F23 | Arrival Delay F57 |
|---|---|---|---|---|
| D1 | 60 min | 30 min | 30 min | 0 min |
| D2 | 60 min | 30 min | 60 min | 60 min |
| D3 | 90 min | 30 min | 90 min | 60 min |

linear segments to the next one (in correspondence to the progressive increase of reference cost functions).

#### 4.2.4. Delay multipliers

Delay multipliers represent the turnaround performance of an airline at a particular airport in case of delayed flights and can be derived from historical flight operations data. A $DM$ is determined as the ratio between departure and arrival delay of the same aircraft, whereby delays are measured as the differences between scheduled and actual times on-blocks. In this case study, $DM$ values are estimated on the basis of publicly available post-ops flight data of the summer season of 2019. Given that airlines have different market shares and partnerships at each airport, also the turnaround performance in case of delays is very heterogeneous (Oreschko et al., 2010). Therefore, the $DM_i$ is an airport- and airline-specific value and depends on the delay of arrival flight $i$. For the definition of these values, only flights from a major German hub carrier with base at Frankfurt airport have been considered which obtained arrival delays between 5 and 90 min. Furthermore, airports have been clustered according to their status in the airline and alliance network, i.e., hub, alliance hub, other hub and other airports. For each airport cluster, observed $DM$ have been mapped and the daily median value is calculated, weighted by the arrival delay first and the aircraft movements during the day second. For instance, Fig. 11 shows the dependency between arrival and departure delay at the airline hub in Frankfurt with the median value $DM = 0.84$ (left) and at other hub airports which are home to a competing (non-alliance) airline with a median value $DM = 1.6$ (right). Table 2 summarizes the defined values for all airport categories. Thus, in case of arrival delays, delays can be compensated at the "own hub", whereas it typically increases at other airports and especially at the hubs of competing airlines due to limited process control ($DM_i > 1$) and congestion. Aside from the airlines' hub, the least reactionary delays are expected at hub airports of alliance partners.

**Table 2**
Delay multipliers per airport category based on historical ground operations data.

| Airport type | Own Hub | Alliance Hub | Other Hub | Other airport |
|---|---|---|---|---|
| Delay multiplier | 0.85 | 1.1 | 1.6 | 1.4 |

### 4.3. Scenario description

In order to compare the recovery performance of all three models (ARM, TRM, IRM) among each other and with the baseline NDM, we induce arrival delays on four different flights (F1, F18, F23, F57) into the morning hub bank. The delays vary in their magnitude as described in Table 1 below, such that we analyse the recovery of three different delay scenarios over the entire day within the rolling horizon algorithm. Thus, if the delay cannot be compensated entirely during the morning hub bank, the remaining delay spreads throughout the airline network and will be back-propagated into the afternoon hub bank, where we apply the recovery models once again (by respecting the altered aircraft assignment in case of aircraft swaps) and follow the same cycle into the evening hub bank, if necessary.

## 5. Analysis

The algorithm was implemented for all four models in a Java environment and solved with IBM CPLEX Version 12.10.0-0 on a 24-core CPU with 64GB RAM. Average solution times per instance are highly dependent on the model type and the number of remaining operations, whereas the complexity of the schedule deviation has only a minor impact. Thus, the longest solution times occur during the morning hub bank with on average: NDM=22 s, TRM=10 min 47 s, ARM=1 h 34 min 44 s, and IRM=29 min 48 s. For the other hub banks, the solution time of each model lies between 5 s and 45 s, while only D2 TRM needed 3 min. Taking into account that we assume an application of our recovery models with at least two hours of Look Ahead Time (LAT) until the first arrival, we still consider these values (especially those for the IRM) as acceptable for a tactical optimization.

The results for each delay scenario are analysed with typical operational Key Performance Indicators (KPIs) of an airline such as:

- total costs (objective)
- total delay/ delay multipliers
- number of missed connections
- number of applied turnaround recovery options
- number of applied aircraft swaps

Thereby, the recovery performance of each model is compared for each KPI against the baseline estimation calculated with the NDM, such that the relative benefit can be compared among all the models. Throughout the entire analysis, it needs to be considered that total costs are the objective of the optimization, while all other KPIs represent only a part of the objective function and, thus, have not been optimized individually. Consequently, their analysis is more exploratory to determine the side effects of optimizing for minimal airline costs.

### 5.1. Delay propagation in the network

As an output of the NDM, Fig. 12 shows the individual delay cost functions for all flights of aircraft 15 within the case study (F23–F27). The graphs illustrate the increasing marginal costs due to the infringement of more and more STWs as well as step costs arising from missed connections in the downstream rotation. Thus, the functions not only contain delay costs for the immediate next flight but also include reactionary costs of delays on all subsequent flights and potentially cancelled connections after them. Note here that the complexity of these functions decreases as the time of day advances, given that fewer downstream interdependencies need to be considered. However, also cumulative buffer times decrease during the course of the day, such that major cost-driving events (such as cost-intensive rebookings with overnight lodging) appear earlier on afternoon and evening flights.

For all functions in the graph on the left, the Delay Multiplier (DM) at all airports in the network is set at $DM = 1.0$ such that arrival delays directly propagate into departure delay, only deducted by the respective ground time buffers. Conversely, the figure on the right shows cost functions with airport-specific DMs as detailed in Table 2. Given that these values are on average above 1, cost functions tend to increase earlier along the $x$-axis, as buffer times on transfer connections are consumed by the multiplicative effect. For validation purposes, both graphs further include a piece-linear cost function which resembles reference delay cost values of the respective aircraft types as determined in Cook (2015). Note that when $DM = 1.0$, the reference cost function shows high similarity with a regression curve of all flights operated by aircraft 15, whereas it underestimates all cost functions when airport-specific DMs are applied.

Fig. 13 shows the cost functions for all flights operated by aircraft 7 (F1–F3) and 13 (F18–F20), whereby airport-specific DMs are applied and one needs to consider that aircraft 13 has a maintenance event scheduled after Flight F20. This means that the flight cycle to Stockholm (ARN) needs to be cancelled once the delay would exceed a critical threshold, which incurs very large costs for rebooking and compensating all passengers on both flights (F19–F20), as can be seen in the graph on the right.

### 5.2. Analysis of delay scenarios

As Fig. 12 and 13 show reactionary delay costs of individual flights, typical delay situations include schedule deviations for more than one aircraft. Therefore, Fig. 14 shows for three (left, F18=30 min, F1 and F23 variable) and four (right, F18=30 min, F57=60 min, F1 and F23 variable) delayed arrival flights the predicted total costs of delay for the entire network. The highlighted circles represent the delay scenarios D1 (left) and D2/D3 (right) from Table 1.

#### 5.2.1. Total costs

Fig. 15 displays total cost results per recovery model for all three delay scenarios. Thereby, each subplot has the character of an event-tree, such that the “NoRecovery Costs” curve (marked in red) includes all costs which would be incurred if no recovery options are applied in none of the three hub banks, while all other curves follow the application of a recovery model in at least one hub bank.

The “NoRecovery Costs” curve is the output of the iterative application of the NDM and represents the baseline (upper bound) of the potential cost spectrum. Note here that the baseline costs estimation made in the morning (which contains downstream cost-drivers for the entire day) is adjusted in each iteration, given that new interdependencies may arise with regard to the ground operations in the upcoming hub bank. Thus, in each iteration, the used MGT, MCT and DM values for the next hub bank in Frankfurt are substituted with scenario-specific stand allocations and corresponding turnaround sub-process and transfer durations (see Section 3.4). Judging from Fig. 15, the baseline adjustment is higher from morning towards afternoon hub banks (on average 7.6% increase) than between afternoon and evening hub banks (on average 0.7% increase). However, it does not increase with the amount of delay but rather seems to depend on the individual network and delay constellation, given that baseline costs in scenario D3 increase only by 4.4%, while in D2 they surge by 13.4%.

The “Optimal Recovery Costs” curve (marked in green) is the result of the continuous application of the respective recovery model in each hub bank. Thus, it represents the minimum (lower bound) of the potential cost spectrum for the given delay scenarios. The corresponding savings are shaded in green, while the areas shaded in red and grey highlight the reduced amount of savings if the models were only applied during the morning or morning+afternoon hub banks. Especially for situations with medium to high delay (see Fig. 15(b) and 15(c)), one can easily recognize that even an (at least partially) recovered schedule deviation can spread over an entire day and may require additional recovery actions in later stages to condemn the resurgence of delay propagation and costs.

Looking into the recovery performance of the individual models, the TRM is most efficient in situations with low to moderate delays. Thereby, in scenario D1 (see Fig. 15(a)) the solution of the TRM resembles the one of the IRM and is able to reduce total costs arising from the given schedule deviation by 49% in the morning hub bank. This is continued by a 8% cost reduction in the afternoon hub bank which results in a full recovery of network performance. Thus, no further recovery actions are required during the evening hub bank aside from a few stand reallocations (see Section 5.2.4). In scenario D2 (see Fig. 15(b)), again the TRM is able to reduce total costs by 49% in the morning, which is followed by 24% in the afternoon and another 28% in the evening so that by the end of the day it performs nearly as well as the ARM. Even in scenario D3 (see Fig. 15(c)), the TRM can save up to 28% of additional costs (and from that another 21% and 16% in the following hub banks), which is however far less than the other two models are able to compensate.

The recovery potential of the ARM in D1 is limited to the extend that departure delays are acceptable above the critical 10-minute threshold to maintain transfer connections. Given the low amount of delay, the option to swap flights between aircraft does not provide any cost savings (see Section 5.2.5), such that additional costs of the given schedule deviation can only be reduced by 25%. With increasing delays on some aircraft rotations, the ARM begins to outperform the TRM, such that in scenario D2 a cost reduction of 56% in comparison to the baseline (roughly 7% more reduction than by TRM) and in situation D3 a 43% cost reduction (15% more than by TRM) can be achieved.

Naturally, the IRM has the best performance of all three recovery models as it combines all available recovery options of the TRM and ARM and trades them off against each other. As mentioned above, aircraft swaps are not efficient in D1, such that the IRM adopts the

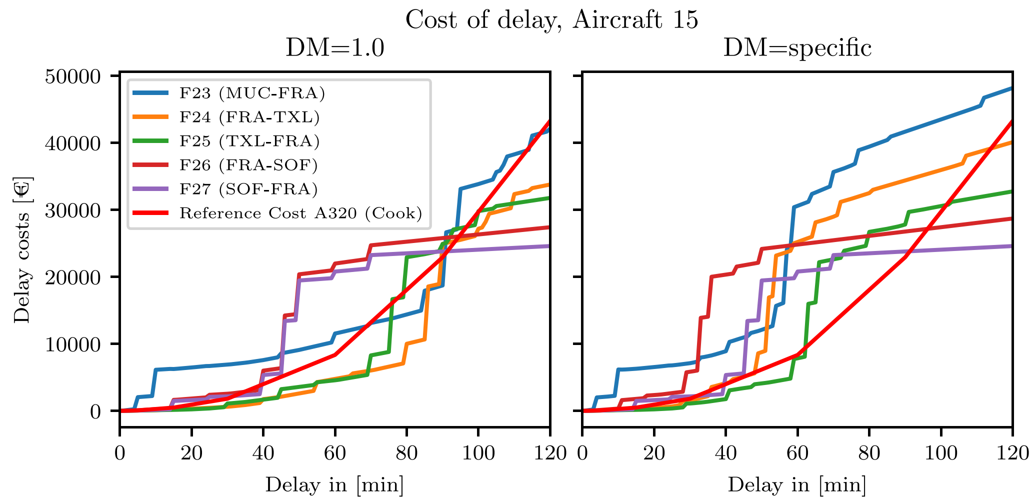


**Fig. 12.** Delay cost functions for departure delays of all flights of aircraft 15 (short-haul). Left: Delay propagates with a DM of 1.0. Right: Stochastic delay propagation with airport-specific DM as specified in Table 2.

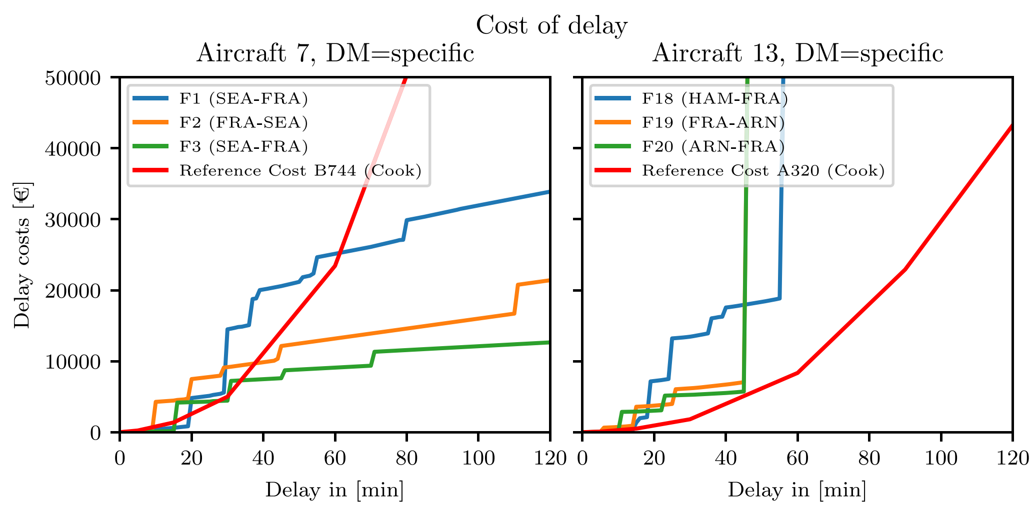


**Fig. 13.** Delay cost functions for aircraft 7 (long-haul) and 13 (short-haul) with airport-specific DM (Table 2).

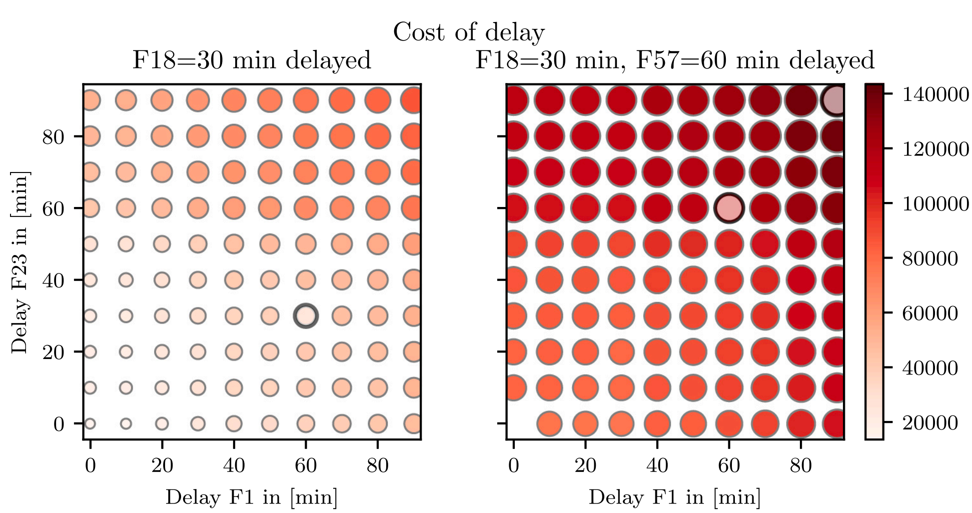


**Fig. 14.** Predicted total costs of delay as a result of three (left) and four (right) delayed arrival flights into the morning hub bank. Three delay scenarios are highlighted for further investigation (D1 left, D2 and D3 right).

**Table 3**
Number of flight delays and their mean duration in optimal solution per scenario.

| # Flight Delays — Duration [h] | D1 | | | D2 | | | D3 | | |
|---|---|---|---|---|---|---|---|---|---|
| | M | A | E | M | A | E | M | A | E |
| NDM | 16 - 6.2 | 17 - 6.6 | 18 - 6.7 | 29 - 25.5 | 27 - 26.2 | 28 - 26.3 | 28 - 30.8 | 31 - 32.5 | 32 - 33.2 |
| TRM | 18 - 6.1 | 20 - 6.5 | 21 - 6.6 | 43 - 23.1 | 47 - 25.9 | 50 - 26.7 | 38 - 27.2 | 46 - 30.1 | 50 - 31.9 |
| ARM | 21 - 7.4 | 21 - 6.5 | 22 - 6.6 | 41 - 25 | 41 - 25 | 42 - 25 | 39 - 32.2 | 45 - 35.1 | 46 - 35.8 |
| IRM | 18 - 6.1 | 20 - 6.5 | 21 - 6.6 | 37 - 17.4 | 36 - 17.7 | 38 - 18 | 37 - 22 | 36 - 22.6 | 41 - 23.4 |

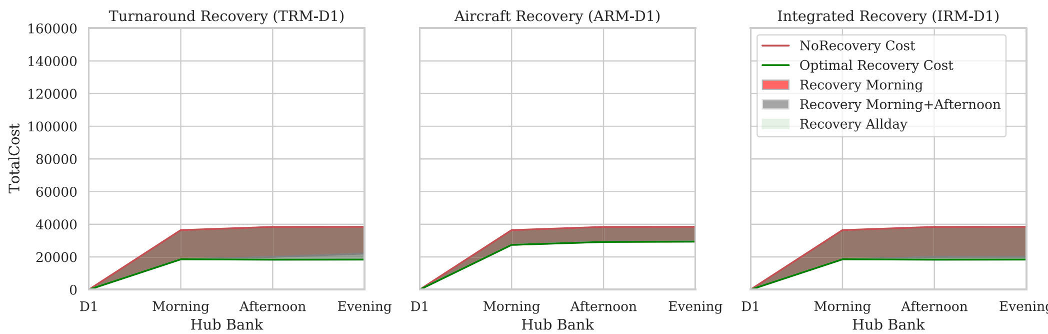


(a) Total costs delay scenario D1.

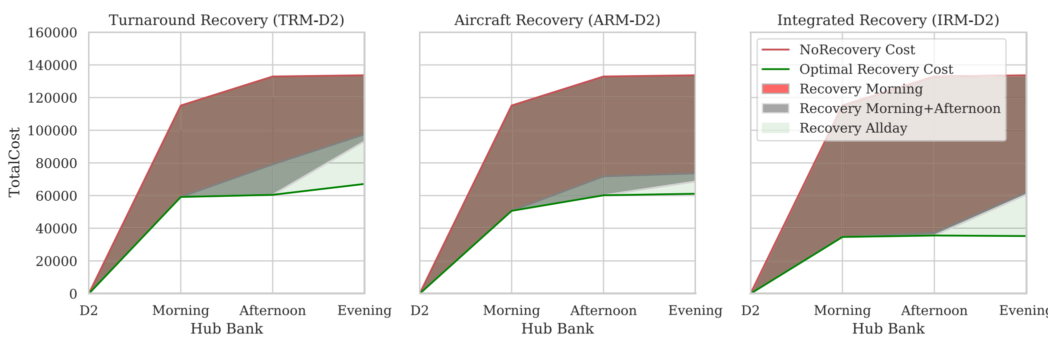


(b) Total costs delay scenario D2.

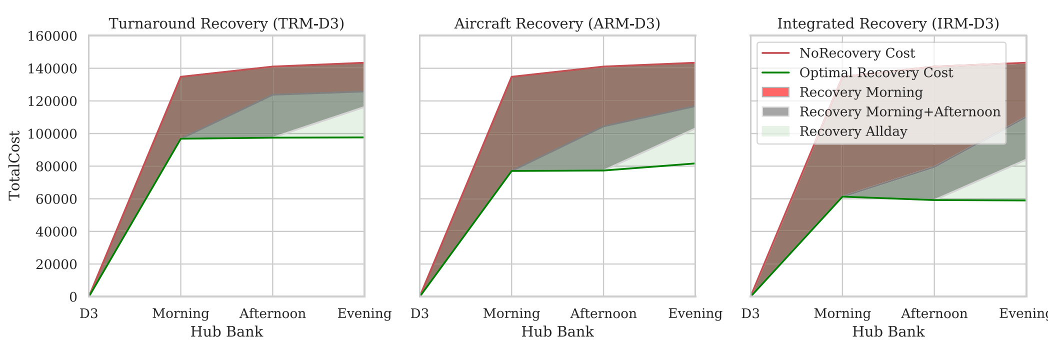


(c) Total costs delay scenario D3.

**Fig. 15.** Total costs per delay scenario and recovery model. Areas shaded in red represent the savings resulting from an application of the respective recovery model during the morning hub bank. Areas shaded in grey display the savings of a morning+afternoon application, while the green shaded area exhibits the recovery savings from a continuous all-day application.

optimal solution from the TRM. In scenario D2, the IRM can reduce costs by 70% in the morning hub bank and another 4% in the afternoon. Based on the optimized ground operations and aircraft flight assignment from the afternoon hub bank, the airport becomes very congested during the evening hub bank. This requires some further recovery actions (especially a reallocation of stands — see Section 5.2.4) in order to save another 42% of additional costs, which would have been incurred from high costs of missed transfer connections at the end of the day. The same applies to scenario D3, with the difference that the IRM can recover a smaller ratio of costs during the morning hub bank (i.e., 55%), such that more actions than in D2 are required during the afternoon and evening hub banks to save another 26% and 30% of total costs.

### 5.2.2. Total delay and delay multiplier

While the average delay per flight decreases within all recovery models, the total delay in the airline network increases in some applications of the ARM and TRM by up to 19% (see Table 3). This ambiguity arises from the fact that both recovery models tend to distribute delay across previously not delayed rotations which have

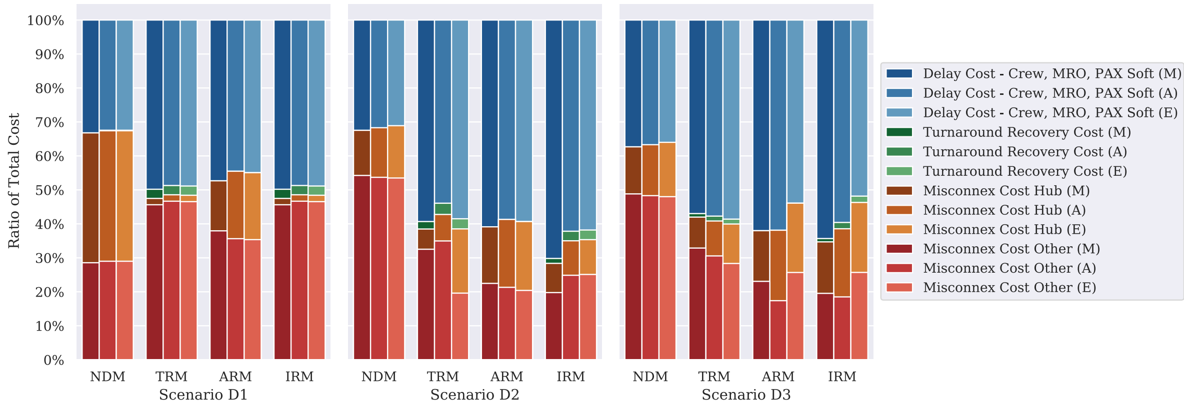


**Fig. 16.** Ratio between delay cost, turnaround recovery cost and misconnex cost at the hub and at other airports.

less critical downstream schedules. An increased number of delayed flights may not be desirable, especially from ATFM perspective, but can be partially compensated by aircraft swaps, such that the ARM, although generating the highest total delay in D2 and D3, is able to contain it within a smaller circle of flights than the TRM. Conversely, the IRM uses the combination of all recovery options for a reduction of delay by 13% per delayed aircraft and in total by 2% in D1 and on average 47% to 44% in D2 and D3 respectively. At the same time, the total delay in both scenarios is reduced by up to 31%.

These results indicate that the applied recovery options are more efficient in terms of reducing delay when the magnitude of a schedule deviation increases. Thereby, the models take into account that re-booking and compensating passengers is often more cost-intensive than assigning minor delays to avoid misconnections (especially during the first delay minutes with marginal costs between 10 and 20 Euro (Cook, 2015)). In D1, the number of delayed flights slightly increases from a baseline of 16 (NDM) up to 21 (with the ARM — see Table 3), whereby the number of aircraft rotations which obtain "official delays" (i.e., above 15-min) increases from formerly three (as defined in the scenario — see Table 1) to four (IRM, TRM) or even five (ARM). In scenarios D2 and D3, four flights induce delays into the network, which results in eleven officially delayed rotations in D2, but only seven in D3. This can be explained with a deeper look into the stand allocation, such that delays around 90 min (in D3) simply cause a reversal of the initial sequence of aircraft at one stand, whereas smaller delays may cause overlapping turnaround periods and stand bottlenecks. Across all scenarios, the IRM generates the fewest delayed rotations of all optimization models, which is preferable in terms of flight schedule continuity. Furthermore, the results show that the delay reduction is most significant in the morning and decreases towards the evening as opportunities for recovery measures and affected flights decrease.

The effect of delay reduction is also indicated through the DM that can be assessed after each turnaround and compared to the assumptions made in Table 2 (especially for those values at the "Own Hub": FRA=0.85) which are considered in the NDM baseline. Thus, a DM update can be calculated per flight or across all flights after each turnaround at the hub and incorporates the added constraints and recovery options of the TRM which relate to ground operations in Frankfurt. These updated values may then be used as new input values for future runs of the NDM (i.e., parameter training). Table 4 summarizes the average post-ops DMs per model and hub bank. Note that these values only relate to rotational delay and do not consider spillover effects to other aircraft. The variation of these values is quite large and it is obvious that they depend very much on the delay situation, time of the day and available recovery options. As expected, DM values are the highest in the NDM, given that rotational delays can only be absorbed by available ground buffers. In turn, the IRM shows the lowest delay propagation over the entire day, especially when considering lower DMs in the evening hub bank of D2 and D3 in comparison to the TRM. This reduction is the consequence of the performed aircraft swaps in the morning which resulted in slightly increased morning values. As noted in Section 5.2.1, there is a full recovery of the network after the afternoon hub bank in D1, such that the afternoon values are very low and no delay propagates from the initial disturbance until the evening.

**Table 4**
Post-ops delay multiplier $DM_i$ (average rotational delay in FRA) in optimal solution.

| Delay multiplier $DM_i$ | D1 | | | D2 | | | D3 | | |
|---|---|---|---|---|---|---|---|---|---|
| | M | A | E | M | A | E | M | A | E |
| NDM | 0.88 | 0.25 | – | 0.92 | 0.85 | 0.87 | 0.98 | 0.71 | 0.87 |
| TRM | 0.77 | 0.25 | – | 0.75 | 0.47 | 1.2 | 0.73 | 0.85 | 1.8 |
| ARM | 0.88 | 0.25 | – | 0.92 | 1.02 | 0.82 | 0.90 | 0.97 | 4.9 |
| IRM | 0.77 | 0.25 | – | 0.76 | 0.52 | 0.02 | 0.92 | 0.65 | 1.4 |

**Table 5**
Post-ops delay multiplier for the entire network. Here, the total delay of all outbound flights and their successors is related to the inbound delay of each hub bank.

| Delay multiplier network | D1 | | | D2 | | | D3 | | |
|---|---|---|---|---|---|---|---|---|---|
| | M | A | E | M | A | E | M | A | E |
| NDM | 2.16 | 0.79 | – | 4.75 | 2.34 | 0.93 | 4.65 | 2.09 | 0.83 |
| TRM | 2.04 | 0.85 | – | 4.27 | 2.39 | 6.5 | 4.4 | 2.98 | 2.7 |
| ARM | 2.69 | 0.59 | – | 2.94 | 1.39 | 0.9 | 2.98 | 1.97 | 2.22 |
| IRM | 2.04 | 0.85 | – | 2.12 | 1.25 | 0.22 | 3.06 | 1.75 | 2.08 |

**Table 6**
Number of missed passenger connections in optimal solution per scenario (total: 417).

| # Misconnex | D1 | | | D2 | | | D3 | | |
|---|---|---|---|---|---|---|---|---|---|
| | M | A | E | M | A | E | M | A | E |
| NDM | 16 | 18 | 18 | 46 | 50 | 50 | 52 | 56 | 57 |
| TRM | 9 | 10 | 10 | 22 | 29 | 29 | 31 | 33 | 32 |
| ARM | 12 | 14 | 14 | 21 | 28 | 28 | 25 | 31 | 34 |
| IRM | 9 | 10 | 10 | 15 | 17 | 17 | 22 | 23 | 25 |

Table 5 summarizes the total delay behaviour with network-wide DMs, which are calculated for each hub bank and delay scenario. Each DM represents the relation of inbound flight delays to total delays on outbound flights and their succeeding flights until the delay is absorbed or the rotation is finished. The value decreases over time, as successively fewer subsequent delays are taken into account. As noted before, a few exceptions arise in the evening scenario, where short inbound delays are lengthened by restrictions during the turnaround. To conclude, the DMs indicate once again that the optimization models mostly reduce the level of delay compared to NDM.

### 5.2.3. Missed connections

A significant cost reduction is attributable to the waiting of flights for passenger connections. Note, as highlighted in the previous section, that this induces only a slight increase of total delay with the TRM and ARM, while the IRM concurrently reduces average and total delay despite waiting for passengers. As enlisted in Table 6, at least 22% in D1 and more than 40% of cancelled connections in D2 and D3 can be recovered if aircraft are allowed to wait more than ten minutes on critically delayed transfer passengers. In D1, the options to assign quick passenger transfers and stand reallocations help the TRM to outperform the ARM and recover four additional connections. However, in scenarios with higher delay, the performance of both models is almost balanced, as the ARM can avoid a high number of misconnections in downstream operations by assigning appropriate aircraft swaps. The IRM, having all recovery options at its disposal, is able to recover between 44% and 66% of all otherwise missed transfers, which corresponds to an increase of the connectivity ratio by roughly 10% to about 95% (i.e., the ratio between missed connections and all connections — 417 in total).

The underlying trade-off between delay costs (which include additional crew wages, maintenance expenses and costs of passenger dissatisfaction) and "Misconnex Costs" is visible in Fig. 16. Therein, the cost ratio attributable to missed connections reduces with the application of all recovery models from about two-thirds to less than half. In D1, local misconnection costs at the hub are almost completely eliminated with the help of the TRM and IRM, while the ARM can only cut them by half (see Section 5.2.1). The ratio between delay costs and costs of missed connections at other airports remains almost unaffected. This changes significantly in D2 and D3 when the application of aircraft swaps breaks the propagation along heavily delayed flight rotations (see Section 5.2.5). Because of these swaps, the IRM has a more balanced share of misconnex costs between the hub and other airports than the TRM. Note that the highest ratio of delay costs in the optimal solution appears in D2, which may be explained by the fact that many transfer connections have buffers around 60 min. Thus, with delays above this threshold, as in scenario D3, many connections can no longer be recovered and result in an increasing share of local misconnex costs (especially in the evening hub bank).

### 5.2.4. Applied turnaround recovery options

Table 7 lists the number of applied turnaround recovery options in the optimal recovery solution. The most notable finding is that no quick-turnaround and quick transfer procedures are applied during the evening hub bank, while, at least in D2 and D3, the initial stand allocation needs to be altered significantly also in the evening (partially due to the assignment of higher departure delays in earlier hub banks). Note that the latter may be different if one would assume a charge per stand reallocation. Generally, the IRM seems to assign less quick-turnaround procedures for a similar or even better solution than the TRM, which again may be explained with the relaxed aircraft rotations as a result of the assigned aircraft swaps (see Section 5.2.5). Note also here that aircraft swaps are assumed with no costs, which may influence the decision process. Conversely, the daily number of quick transfers and stand changes is almost even between both models.

### 5.2.5. Applied aircraft swaps

Table 8 exhibits the number of aircraft swaps in the optimal recovery solution. While the delay in scenario D1 does not require any swaps, additional 30 min of arrival delay on F23 and 60 min of arrival delay on F57 in scenario D2 are recovered with nine aircraft swaps when only the ARM is applied. The application of the IRM renders two aircraft swaps unnecessary, while the remaining seven swaps remain equal. Also in scenario D3, the same nine swaps are comprised in the optimal recovery solution of the ARM, while the IRM cannot change this result any longer. Consequently, a solution with nine aircraft swaps seems to be a stable output for the given delay constellation.

**Table 7**
Number of applied turnaround recovery options in optimal solution per scenario.

| Scenario ID/ Model | # Quick Turnaround | | | # Quick Transfer | | | # Stand Reallocation | | |
|---|---|---|---|---|---|---|---|---|---|
| | M | A | E | M | A | E | M | A | E |
| D1/ TRM | 1 | 0 | 0 | 2 | 0 | 0 | 10 | 7 | 4 |
| D1/ IRM | 1 | 0 | 0 | 2 | 0 | 0 | 9 | 5 | 5 |
| D2/ TRM | 3 | 2 | 0 | 4 | 1 | 0 | 8 | 9 | 4 |
| D2/ IRM | 1 | 1 | 0 | 2 | 2 | 0 | 10 | 7 | 8 |
| D3/ TRM | 2 | 1 | 0 | 4 | 1 | 0 | 10 | 7 | 8 |
| D3/ IRM | 1 | 1 | 0 | 3 | 2 | 0 | 11 | 7 | 8 |

**Table 8**
Number of aircraft swaps in the optimal recovery solution of each model.

| # Aircraft swaps | D1 | D2 | D3 |
|---|---|---|---|
| TRM | – | – | – |
| ARM | 0 | 9 | 9 |
| IRM | 0 | 7 | 9 |

Note that we do not consider any administrative charge for aircraft swaps, such that these decisions are mainly triggered by delay propagation effects and connectivity decisions (e.g., an aircraft may obtain additional departure delay to maintain a critical transfer connection, which also impacts its downstream rotation, such that some flights are swapped to other aircraft). Further note that in our network layout, one swap can only be initiated at the hub airport and includes two flight legs (towards an out-station and back, whereby for evening flights the second leg may be on the next day). Considering the small long-haul fleet in our example (two aircraft during the morning and evening hub banks), aircraft swaps are more likely to occur on continental flights.

## 6. Conclusion and discussion

We integrated an extended RCPSP into an aircraft routing model to incorporate the aircraft turnaround – assumed to be one of the major contributors to airline delay – and its related recovery potential into existing solutions for integrated aircraft, crew, and passenger recovery. Our approach fills a research gap on decision support across multiple AOCC departments as it provides a way forward for the prediction of delay propagation in airline networks and its optimal recovery along the daily trajectory of an aircraft (considering flight and ground interdependencies).

The basic network delay model (NDM) is able to validate step-linear delay cost functions (previously introduced in Pilon et al. (2016), Evler et al. (2020)) as flight- and airline-specific alternatives to statistically-fitted reference delay cost functions (Cook, 2015). For flights that are operated later in the day, we find that the complexity of such functions decreases while cost-driving downstream events (cost steps) occur with less buffer time. The buffer times until critical events are further influenced by airport-specific delay multipliers. These describe whether incoming delays can be compensated at downstream airports or whether additional rotational delays need to be considered after the respective ground segment. In the presented research, we include delay multipliers which are derived from aggregating historical turnaround data. However, during the deployment in an operational environment, these model parameters could also be learned and continuously adjusted from an airport- to a flight-specific level. In fact, the implementation of the integrated recovery model into a dynamic optimization algorithm with a rolling horizon has highlighted that initial costs and delay estimations need to be updated every time when generalized transition times (e.g., MCT and MGT) are substituted with specific constraints related to ground operations.

The recovery performance within a dynamic algorithm is compared between the integrated model (IRM) and the individual turnaround

(TRM) and aircraft recovery models (ARM). In the context of a case study, various delay scenarios are applied, covering a day of operations for 17 aircraft at the hub airport Frankfurt. The results reveal that the TRM is most efficient in low and moderate delay situations and especially during the morning hub bank, given that delays can be contained before they propagate through the network. This reduces total costs in comparison to the conventional ARM by up to 49% and enables full recovery of the flight schedule without often considered recovery options such as aircraft swaps or flight cancellations. Although the local turnaround recovery potential may be limited to inbound delays above 30 min in our case study, the additional flexibility during ground operations still complements aircraft recovery options and increases the resilience of the airline network. Thus, in medium and high delay scenarios, the IRM is able to generate additional cost savings of at least 21% in comparison to the ARM. Concurrently, total and average delay, as well as the necessary amount of optimal recovery options, are reduced. Thereby, we observe that delays are primarily distributed to non-critical and previously unaffected rotations. Future research may need to evaluate whether this strategy aligns with the seasonal slot performance, potential ATFM regulations as in Evler et al. (2021b) and the overall efficiency of the ATM network (especially if multiple airlines were to apply similar principles in parallel).

We envision the application of our approach within a tactical setting with a rolling horizon, i.e., with a look-ahead time of at least two hours prior to the first arrival of each hub bank. The continuous application before each hub bank is advisable in order to prevent the resurgence of costs and propagation effects that relate to the reactionary delay of the previous hub bank. Although current solution times with standard solvers seem appropriate to demonstrate the feasibility of this concept, further consideration should be given to get closer to a real-time setting. This would especially be the case if one wants to compare the performance of our approach to large-scale and/or multi-hub airline networks with up to 1100 flights as analysed in Abdelghany et al. (2008), Petersen et al. (2012b), Maher (2016). While the scalability of our approach is given, solution times strongly depend on the size of the network instance, such that the proposed LP formulation should be tightened or the problem should be migrated into an appropriate heuristic solution technique.

Aside from the tactical setting, the model can be used to check the efficiency of flight schedules and recovery policies in the strategic planning stage. Strategic schedules currently contain longer ground buffers during the evening hub bank which aim at minimizing night curfew infringements and high rebooking and compensation costs once passengers would miss the last flight of the day. In our scenarios, these extended ground times create congestion at the hub during the evening hours, given that more stands are occupied in parallel, which is enforced by higher departure delays to await critical connections. Thus, high ground buffers seem to make extra resources dedicated to turnaround recovery obsolete, such that airlines should double-check how many reserve capacities they provide per hub bank (see the concept of recoverable robustness introduced in Liebchen et al. (2009), Vink et al. (2020)).

## CRediT authorship contribution statement

**Jan Evler:** Conceptualization, Data curation, Formal analysis, Investigation, Methodology, Software, Validation, Visualization, Writing – original draft, Writing – review & editing. **Martin Lindner:** Conceptualization, Data curation, Formal analysis, Investigation, Methodology, Software, Validation, Visualization, Writing – original draft. **Hartmut Fricke:** Conceptualization, Funding acquisition, Supervision, Project administration. **Michael Schultz:** Conceptualization, Supervision, Writing – review & editing.

## Acknowledgements

We thank our colleagues from the Department of Data Science at the F. A. University Erlangen–Nuremberg for their suggestion on the mathematical model.

This project has received funding from the German Federal Ministry of Economic Affairs and Energy (BMWI) within the LUFO-V grant agreement No. 20X1711M (OPsTIMAL). Further funding was received from the SESAR Joint Undertaking under the European Union's Horizon 2020 research and innovation programme under grant agreement No. 783287 (Engage KTN). The opinions expressed herein reflect the authors' views only. Under no circumstances shall the SESAR Joint Undertaking be responsible for any use that may be made of the information contained herein.

## References

Abdelghany, K.F., Abdelghany, A.F., Ekollu, G., 2008. An integrated decision support tool for airlines schedule recovery during irregular operations. European J. Oper. Res. 185 (2), 825–848. http://dx.doi.org/10.1016/j.ejor.2006.12.045.

Abdelghany, A., Ekollu, G., Narasimhan, R., Abdelghany, K., 2004. A proactive crew recovery decision support tool for commercial airlines during irregular operations. Ann. Oper. Res. 127 (1–4), 309–331. http://dx.doi.org/10.1023/B:ANOR.0000019094.19940.41.

AhmadBeygi, S., Cohn, A., Guan, Y., Belobaba, P., 2008. Analysis of the potential for delay propagation in passenger airline networks. J. Air Transp. Manag. 14 (5), 221–236. http://dx.doi.org/10.1016/j.jairtraman.2008.04.010.

AhmadBeygi, S., Cohn, A., Lapp, M., 2010a. Decreasing airline delay propagation by re-allocating scheduled slack. IIE Trans. 42 (7), 478–489. http://dx.doi.org/10.1080/07408170903468605.

AhmadBeygi, S., Cohn, A., Lapp, M., 2010b. Decreasing airline delay propagation by re-allocating scheduled slack. IIE Trans. 42 (7), 478–489. http://dx.doi.org/10.1080/07408170903468605.

Ali, H., Guleria, Y., Alam, S., Schultz, M., 2019. A passenger-centric model for reducing missed connections at low cost airports with gates reassignment. IEEE Access 7, 179429–179444. http://dx.doi.org/10.1109/ACCESS.2019.2953769, Conference Name: IEEE Access.

Aloulou, M.A., Haouari, M., Zeghal Mansour, F., 2010. Robust aircraft routing and flight retiming. Electron. Notes Discrete Math. 36 (C), 367–374. http://dx.doi.org/10.1016/j.endm.2010.05.047.

Aloulou, M.A., Haouari, M., Zeghal Mansour, F., 2013. A model for enhancing robustness of aircraft and passenger connections. Transp. Res. C 32, 48–60. http://dx.doi.org/10.1016/j.trc.2013.03.008.

Andersson, T., Värbrand, P., 2004. The flight perturbation problem. Transp. Plan. Technol. 27 (2), 91–117. http://dx.doi.org/10.1080/0308106042000218195.

Arikan, U., Gürel, S., Aktürk, M.S., 2016. Integrated aircraft and passenger recovery with cruise time controllability. Ann. Oper. Res. 236, 295–317.

Atkinson, S.E., Ramdas, K., Williams, J.W., 2016. Robust scheduling practices in the US airline industry: Costs, returns, and inefficiencies. Manage. Sci. 62 (11), 3372–3391.

Ball, M., Barnhart, C., Nemhauser, G., Odoni, A., 2007. Air transportation: Irregular operations and control. In: Handbooks in Operations Research and Management Science, Vol. 14. pp. 1–67.

Bard, J.F., Yu, G., Arguello, M.F., 2001. Optimizing aircraft routings in response to groundings and delays. IIE Trans. 33 (10), 931–947. http://dx.doi.org/10.1080/07408170108936885.

Bratu, S., Barnhart, C., 2006. Flight operations recovery: New approaches considering passenger recovery. J. Sched. 9 (3), 279–298. http://dx.doi.org/10.1007/s10951-006-6781-0.

Bryan, D.L., O'Kelly, M.E., 1999. Hub-and-spoke networks in air transportation: An analytical review. J. Reg. Sci. 39 (2), 275–295. http://dx.doi.org/10.1111/1467-9787.00134.

Burke, E.K., De Causmaecker, P., De Maere, G., Mulder, J., Paelinck, M., Vanden Berghe, G., 2010. A multi-objective approach for robust airline scheduling. Comput. Oper. Res. 37 (5), 822–832. http://dx.doi.org/10.1016/j.cor.2009.03.026.

Castro, A.J.M., Oliveira, E., 2011. A new concept for disruption management in airline operations control. Proc. Inst. Mech. Eng. G 225 (3), 269–290. http://dx.doi.org/10.1243/09544100JAERO864.

Clausen, J., Larsen, A., Larsen, J., Rezanova, N.J., 2010. Disruption management in the airline industry—Concepts, models and methods. Comput. Oper. Res. 37 (5), 809–821. http://dx.doi.org/10.1016/j.cor.2009.03.027.

Cook, A., 2015. European Airline Delay Cost Reference Values - Updated and Extended Values. Technical Report 4.1, University of Westminster, London, p. 110.

Cook, A., Tanner, G., 2015. The Cost of Passenger Delay to Airlines in Europe. Consultantion Document, University of Westminster, London.

Cook, A., Tanner, G., Williams, V., Meise, G., 2009. Dynamic cost indexing – managing airline delay costs. J. Air Transp. Manag. 15 (1), 26–35. http://dx.doi.org/10.1016/j.jairtraman.2008.07.001.

Cordeau, J.-F., 2000. The VRP with Time Windows. Groupe d'études et de recherche en analyse des décisions Montréal.

Deblaere, F., Demeulemeester, E., Herroelen, W., 2011. Reactive scheduling in the multi-mode RCPSP. Comput. Oper. Res. 38 (1), 63–74. http://dx.doi.org/10.1016/j.cor.2010.01.001.

Delgado, L., Martin, J., Blanch, A., Cristóbal, S., 2016. Hub operations delay recovery based on cost optimisation. In: 6th SESAR Innovation Days. Delft, p. 11.

Dijk, B., Santos, B.F., Pita, J.P., 2019. The recoverable robust stand allocation problem: A GRU airport case study. OR Spectrum 41 (3), 615–639. http://dx.doi.org/10.1007/s00291-018-0525-3.

Du, J.Y., Brunner, J.O., Kolisch, R., 2014. Planning towing processes at airports more efficiently. Transp. Res. E: Logist. Transp. Rev. 70, 293–304. http://dx.doi.org/10.1016/j.tre.2014.07.008.

Dück, V., Ionescu, L., Kliewer, N., Suhl, L., 2012. Increasing stability of crew and aircraft schedules. Transp. Res. C 20 (1), 47–61. http://dx.doi.org/10.1016/j.trc.2011.02.009.

Dunbar, M., Froyland, G., Wu, C.-L., 2014. An integrated scenario-based approach for robust aircraft routing, crew pairing and re-timing. Comput. Oper. Res. 45, 68–86. http://dx.doi.org/10.1016/j.cor.2013.12.003.

Eggenberg, N., Salani, M., Bierlaire, M., 2010. Constraint-specific recovery network for solving airline recovery problems. Comput. Oper. Res. 37 (6), 1014–1026. http://dx.doi.org/10.1016/j.cor.2009.08.006.

El-Sherbeny, N.A., 2010. Vehicle routing with time windows: An overview of exact, heuristic and metaheuristic methods. J. King Saud Univ. - Sci. 22 (3), 123–131. http://dx.doi.org/10.1016/j.jksus.2010.03.002.

Eurocontrol, 2018. Airport Network Integration - Concept for establishment of an Airport Operations Plan (AOP). Technical Report, Eurocontrol.

Eurocontrol, 2020. PRR 2019 - Performance Review Report. Technical Report, Eurocontrol, Brussels, http://dx.doi.org/10.1163/1570-6664, type: dataset.

Evler, J., Asadi, E., Preis, H., Fricke, H., 2021a. Airline ground operations: Schedule recovery optimization approach with constrained resources. Transp. Res. C 128, http://dx.doi.org/10.1016/j.trc.2021.103129.

Evler, J., Schultz, M., Fricke, H., 2021b. Flight prioritization and turnaround recovery. In: 14th ATM Research and Development Seminar. online, p. 10.

Evler, J., Schultz, M., Fricke, H., Cook, A., 2020. Development of stochastic delay cost functions. In: 10th SESAR Innovation Days. online, p. 9.

Fricke, H., Schultz, M., 2009. Delay impacts onto turnaround performance. In: 8th USA/Europe Air Traffic Management Research and Development Seminar. ATM2009, p. 10.

Gupta, P., Sargut, F., Ahuja, R., Bolia, N., 2018. OTP maximizer: Robust airline scheduling with optimal block and ground times.

Hu, Y., Song, Y., Zhao, K., Xu, B., 2016. Integrated recovery of aircraft and passengers after airline operation disruption based on a GRASP algorithm. Transp. Res. E: Logist. Transp. Rev. 87, 97–112. http://dx.doi.org/10.1016/j.tre.2016.01.002.

Kohl, N., Larsen, A., Larsen, J., Ross, A., Tiourine, S., 2007. Airline disruption management—Perspectives, experiences and outlook. J. Air Transp. Manag. 13 (3), 149–162. http://dx.doi.org/10.1016/j.jairtraman.2007.01.001.

Kuster, J., Jannach, D., Friedrich, G., 2009. Extending the RCPSP for modeling and solving disruption management problems. Appl. Intell. 31 (3), 234–253. http://dx.doi.org/10.1007/s10489-008-0119-x.

Lettovsky, L., 1997. Airline Operations Recovery: An Optimization Approach (Ph.D. thesis). Georgia Institute of Technology.

Lettovský, L., Johnson, E.L., Nemhauser, G.L., 2000. Airline crew recovery. Transp. Sci. 34 (4), 337–348. http://dx.doi.org/10.1287/trsc.34.4.337.12316.

Liang, Z., Xiao, F., Qian, X., Zhou, L., Jin, X., Lu, X., Karichery, S., 2018. A column generation-based heuristic for aircraft recovery problem with airport capacity constraints and maintenance flexibility. Transp. Res. B 113, 70–90. http://dx.doi.org/10.1016/j.trb.2018.05.007.

Liebchen, C., Lübbecke, M., Möhring, R., Stiller, S., 2009. The concept of recoverable robustness, linear programming recovery, and railway applications. In: Lecture Notes in Computer Science, vol. 5868, p. 439.

Lonzius, M.C., Lange, A., 2017. Robust scheduling: An empirical study of its impact on air traffic delays. Transp. Res. E: Logist. Transp. Rev. 100, 98–114. http://dx.doi.org/10.1016/j.tre.2016.12.012.

Løve, M., Sørensen, K.R., Larsen, J., Clausen, J., 2002. Disruption management for an airline — Rescheduling of aircraft. In: Cagnoni, S., Gottlieb, J., Hart, E., Middendorf, M., Raidl, G.R. (Eds.), Applications of Evolutionary Computing. Springer Berlin Heidelberg, Berlin, Heidelberg, pp. 315–324.

Maher, S.J., 2016. Solving the integrated airline recovery problem using column-and-row generation. Transp. Sci. 50 (1), 216–239.

Marla, L., Vaaben, B., Barnhart, C., 2017. Integrated disruption management and flight planning to trade off delays and fuel burn. Transp. Sci. 51 (1), 88–111. http://dx.doi.org/10.1287/trsc.2015.0609.

Mazzarisi, P., Zaoli, S., Lillo, F., Delgado, L., Gurtner, G., Cook, A., Valput, D., 2019. Network-wide assessment of 4D trajectory adjustments using an agent-based model. In: 9th SESAR Innovation Days. Athens, p. 8.

Medard, C.P., Sawhney, N., 2007. Airline crew scheduling from planning to operations. European J. Oper. Res. 183 (3), 1013–1027. http://dx.doi.org/10.1016/j.ejor.2005.12.046.

Nasiri, M.M., 2013. A pseudo particle swarm optimization for the RCPSP. Int. J. Adv. Manuf. Technol. 65 (5–8), 909–918. http://dx.doi.org/10.1007/s00170-012-4227-8.

Oreschko, B., Kunze, T., Schultz, M., Fricke, H., Kumar, V., Sherry, L., 2012. Turnaround prediction with stochastic process times and airport specific delay pattern. In: 5th International Conference for Research in Air Transportation (ICRAT2012), ICRAT, pp. 9.

Oreschko, B., Schultz, M., Elflein, J., Fricke, H., 2010. Significant turnaround process variations due to airport characteristics. In: Proceedings of the First International Air Transport and Operations Symposium 2010, ATOS, Delft.

Padrón, S., Guimarans, D., Ramos, J.J., Fitouri-Trabelsi, S., 2016. A bi-objective approach for scheduling ground-handling vehicles in airports. Comput. Oper. Res. 71, 34–53. http://dx.doi.org/10.1016/j.cor.2015.12.010.

Petersen, J.D., Sölveling, G., Clarke, J.P., Johnson, E.L., Shebalov, S., 2012a. An optimization approach to airline integrated recovery. Transp. Sci. 46 (4), 482–500. http://dx.doi.org/10.1287/trsc.1120.0414.

Petersen, J.D., Sölveling, G., Clarke, J.-P., Johnson, E.L., Shebalov, S., 2012b. An optimization approach to airline integrated recovery. Transp. Sci. 46 (4), 482–500. http://dx.doi.org/10.1287/trsc.1120.0414.

Pilon, N., Cook, A., Ruiz, S., Bujor, A., Castelli, L., 2016. Improved flexibility and equity for airspace users during demand-capacity imbalance. In: 6th SESAR Innovation Days. Delft, p. 8.

Rosenberger, J.M., Johnson, E.L., Nemhauser, G.L., 2003. Rerouting aircraft for airline recovery. Transp. Sci. 37 (4), 408–421. http://dx.doi.org/10.1287/trsc.37.4.408.23271.

Rosenberger, J.M., Johnson, E.L., Nemhauser, G.L., 2004. A robust fleet-assignment model with hub isolation and short cycles. Transp. Sci. 38 (3), 357–368. http://dx.doi.org/10.1287/trsc.1030.0038.

Rosenberger, J.M., Schaefer, A.J., Goldsman, D., Johnson, E.L., Kleywegt, A.J., Nemhauser, G.L., 2002. A stochastic model of airline operations. Transp. Sci. 36 (4), 357–377. http://dx.doi.org/10.1287/trsc.36.4.357.551.

Safak, O., Gürel, S., Aktürk, M.S., 2017. Integrated aircraft-path assignment and robust schedule design with cruise speed control. Comput. Oper. Res. 84, 127–145. http://dx.doi.org/10.1016/j.cor.2017.03.005.

Santos, B.F., Wormer, M.M., Achola, T.A., Curran, R., 2017. Airline delay management problem with airport capacity constraints and priority decisions. J. Air Transp. Manag. 63, 34–44. http://dx.doi.org/10.1016/j.jairtraman.2017.05.003.

Schlegel, A., 2010a. Bodenabfertigungsprozesse Im Luftverkehr: Eine Statistische Analyse Am Beispiel Der Deutschen Lufthansa AG Am Flughafen Frankfurt/Main. Gabler Verlag.

Schlegel, A., 2010b. Bodenabfertigung. In: Bodenabfertigungsprozesse Im Luftverkehr. Gabler, pp. 47–76. http://dx.doi.org/10.1007/978-3-8349-8691-7_3.

Schultz, M., 2018a. Field trial measurements to validate a stochastic aircraft boarding model. Aerospace 5 (1), 27. http://dx.doi.org/10.3390/aerospace5010027.

Schultz, M., 2018b. Implementation and application of a stochastic aircraft boarding model. Transp. Res. C 90, 334–349. http://dx.doi.org/10.1016/j.trc.2018.03.016.

Sinclair, K., Cordeau, J.-F., Laporte, G., 2014. Improvements to a large neighborhood search heuristic for an integrated aircraft and passenger recovery problem. European J. Oper. Res. 233 (1), 234–245. http://dx.doi.org/10.1016/j.ejor.2013.08.034.

Sinclair, K., Cordeau, J.-F., Laporte, G., 2016a. A column generation post-optimization heuristic for the integrated aircraft and passenger recovery problem. Comput. Oper. Res. 65, 42–52. http://dx.doi.org/10.1016/j.cor.2015.06.014.

Sinclair, K., Cordeau, J.-F., Laporte, G., 2016b. A column generation post-optimization heuristic for the integrated aircraft and passenger recovery problem. Comput. Oper. Res. 65, 42–52. http://dx.doi.org/10.1016/j.cor.2015.06.014.

Sohoni, M., Lee, Y.C., Klabjan, D., 2011. Robust airline scheduling under block-time uncertainty. Transp. Sci. 45 (4), 451–464. http://dx.doi.org/10.1287/trsc.1100.0361.

Stojkovic, M., Soumis, F., 2005. The operational flight and multi-crew scheduling problem. Yugosl. J. Oper. Res. 15 (1), 25–48. http://dx.doi.org/10.2298/YJOR0501025S.

Stojković, G., Soumis, F., Desrosiers, J., Solomon, M.M., 2002. An optimization model for a real-time flight scheduling problem. Transp. Res. A 36 (9), 779–788. http://dx.doi.org/10.1016/S0965-8564(01)00039-8.

Thengvall, B.G., Bard, J.F., Yu, G., 2000. Balancing user preferences for aircraft schedule recovery during irregular operations. IIE Trans. 32 (3), 181–193. http://dx.doi.org/10.1023/A:1007618928820.

Tomasella, M., Clare, A., Gök, Y.S., Guimarans, D., Ozturk, C., 2019. Sttar: A simheuristics-enabled scheme for multi-stakeholder coordination of aircraft turnaround operations. In: 2019 Winter Simulation Conference. WSC, pp. 488–499. http://dx.doi.org/10.1109/WSC40007.2019.9004787, ISSN: 0891-7736.

Vidosavljevic, A., Tosic, V., 2010. Modeling of turnaround process using Petri nets. In: Air Transport Research Society (ATRS) World Conference. Air Transport Research Society, Porto, Portugal.

Vink, J., Santos, B., Verhagen, W., Medeiros, I., Filho, R., 2020. Dynamic aircraft recovery problem - an operational decision support framework. Comput. Oper. Res. 117, 104892. http://dx.doi.org/10.1016/j.cor.2020.104892.

Wu, C.-L., 2006. Improving airline network robustness and operational reliability by sequential optimisation algorithms. Netw. Spat. Econ. 6 (3–4), 235–251. http://dx.doi.org/10.1007/s11067-006-9282-y.

Wu, C.-L., 2016. Airline Operations and Delay Management: Insights from Airline Economics, Networks and Strategic Schedule Planning. RA7PCwAAQBAJ, Routledge, Google-Books-ID.

Wu, C.-L., Caves, R.E., 2004. Modelling and simulation of aircraft turnaround operations at airports. Transp. Plan. Technol. 27 (1), 25–46. http://dx.doi.org/10.1080/0308106042000184445.

Wu, C.-L., Law, K., 2019. Modelling the delay propagation effects of multiple resource connections in an airline network using a Bayesian network model. Transp. Res. E: Logist. Transp. Rev. 122, 62–77. http://dx.doi.org/10.1016/j.tre.2018.11.004.

Xu, Y., Wandelt, S., Sun, X., 2019. Stochastic tail assignment under recovery. In: Thirteenth USA/Europe Air Traffic Management Research and Development Seminar. ATM2019.

Yan, C., Kung, J., 2018. Robust aircraft routing. Transp. Sci. 52 (1), 118–133. http://dx.doi.org/10.1287/trsc.2015.0657.

Yan, S., Yang, D.-H., 1996. A decision support framework for handling schedule perturbation. Transp. Res. B 30 (6), 405–419. http://dx.doi.org/10.1016/0191-2615(96)00013-6.

Yang, T., Hu, Y., 2019. Considering passenger preferences in integrated postdisruption recoveries of aircraft and passengers. Math. Probl. Eng. 2019, 1–19. http://dx.doi.org/10.1155/2019/9523610.

Zhang, D., Lau, H.H., Yu, C., 2015. A two stage heuristic algorithm for the integrated aircraft and crew schedule recovery problems. Comput. Ind. Eng. 87, 436–453.